Comparative energetic particle environments in the solar system

N. Krupp

Max-Planck-Institut für Sonnensystemforschung

Max-Planck-Str. 2, 37191 Katlenburg-Lindau, Germany

new address from 2014 on:

Justus-von-Liebig-Weg 3, 37077 Göttingen, Germany

Outline

A. Introduction
B. Energetic particles from the Sun
C. Energetic particles in interplanetary space
D. Particles from Interstellar space
E. Energetic particles in planetary magnetospheres

A. Introduction

1. Energetic particle sources
2. Motion of charged particles in a magnetic field
3. Characteristic parameters
4. Instrumentation to measure energetic particles

A.1 Sources of energetic particles

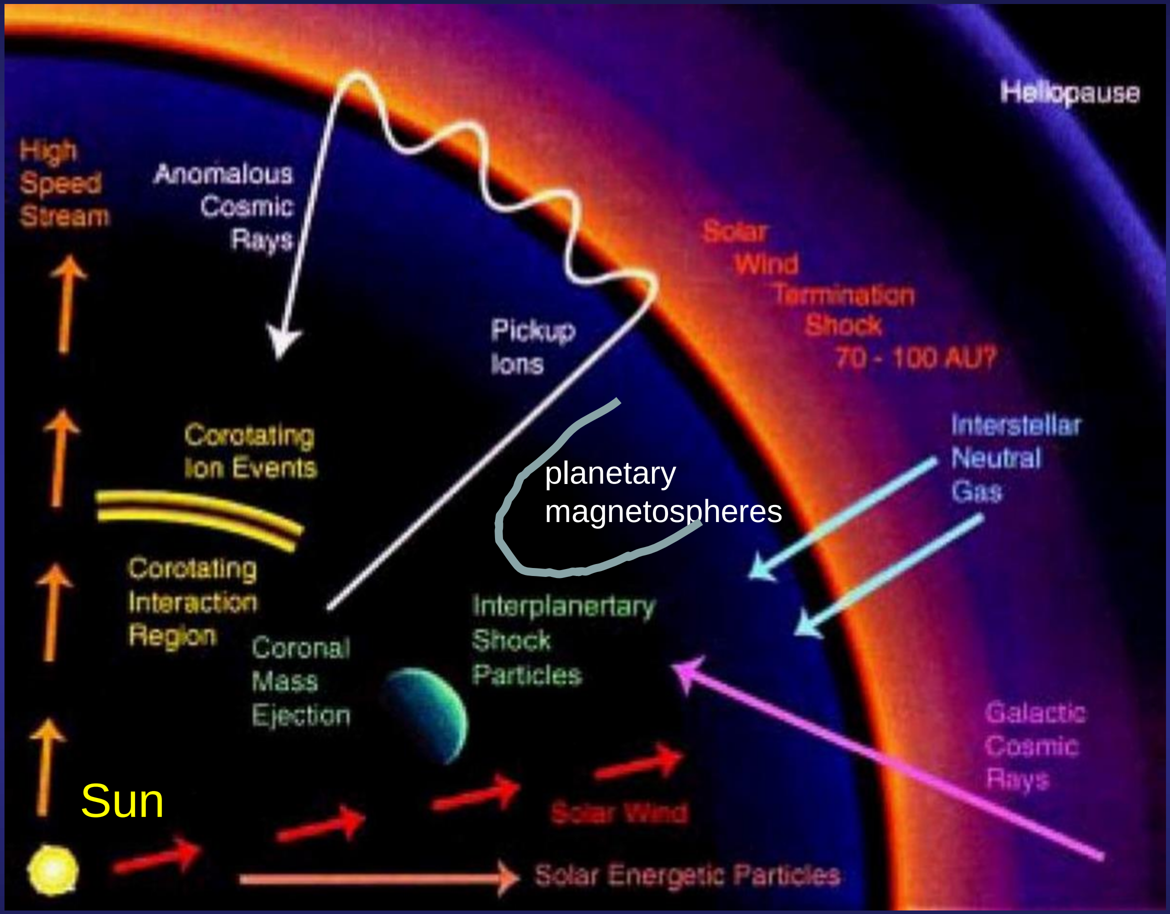

Energetic particles in the heliosphere can be of

- extra-galactic
- galactic
- solar
- planetary

origin

and cover an energy range from 1eV to more 10^{20}eV (eV=electron volt=energy gain of electron in 1 Volt potential)

Particle types

- Electrons
- charged atoms
- charged molecules
- neutral atoms
- neutral molecules
- dust

A. Introduction
Motivation tu study energetic particles

Eneregetic particles are a very useful tool to study

- **Fundamental physics**
- **plasma physics**
- **acceleration mechanisms**
- **geochemistry and solar system evolution,**
- **atmospheric composition and evolution**
- **magnetospheric dynamics...**

A.2: Particle motion
Adiabatic invariants

first adiabatic invariant μ *:*

$$\mu_B = \frac{p_\perp^2}{2m_0B} = const \quad with\ p_\perp = mv\sin\alpha$$

α : pitch angle

angle between the direction of the particle and the magnetic field

second adiabatic invariant J :

$$J = 2\int_{x_m}^{x_{m'}} p_{\|}ds = const \qquad (or\ \ K = \frac{J}{2\sqrt{m_0\mu_B}})$$

third adiabatic invariant Φ_B *:*

$$\Phi_B = \oint Bds = constant$$

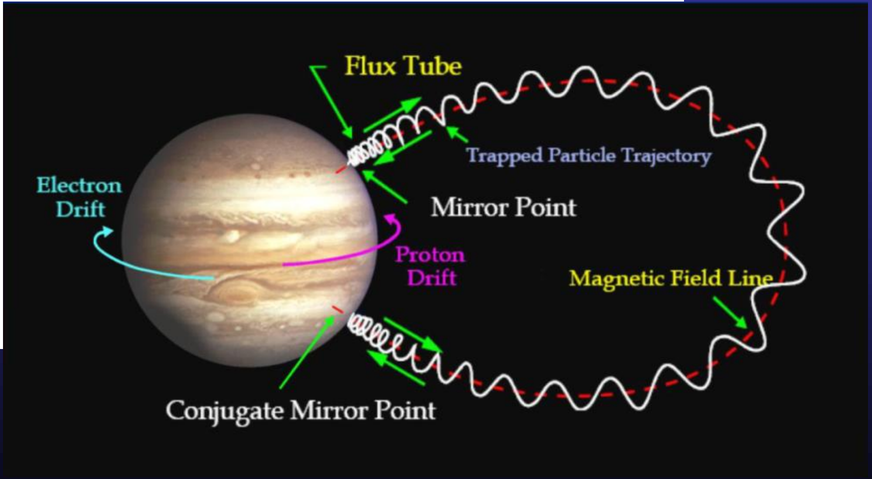

A.2: Particle motion
Particle drifts

$$\vec{V}_E = \frac{\vec{E} \times \vec{B}}{B^2}$$

$$\vec{V}_G = \frac{mv_\perp^2}{2qB^3}(\vec{B} \times \nabla B)$$

$$\vec{V}_C = \frac{mv_\parallel^2}{qB^3}(\vec{B} \times \nabla B)$$

$$\vec{V}_\perp = \vec{V}_E + \vec{V}_G + \vec{V}_C = \frac{\vec{E} \times \vec{B}}{B^2} + \frac{m}{qB^3}(\frac{v_\perp^2}{2} + v_\parallel^2)\vec{B} \times \nabla B$$

A.2: Motion of charged particles
Pickup process

Illustration of the classical picture of ion pickup in perpendicular electric $E = -V_{sw} \times B$ and magnetic B fields. Ions moving on the cycloidal trajectory oscillate between zero and $2V_{sw}$ velocities, while the gyrocenter moves at V_{sw}. The ion in this case is initially at rest.

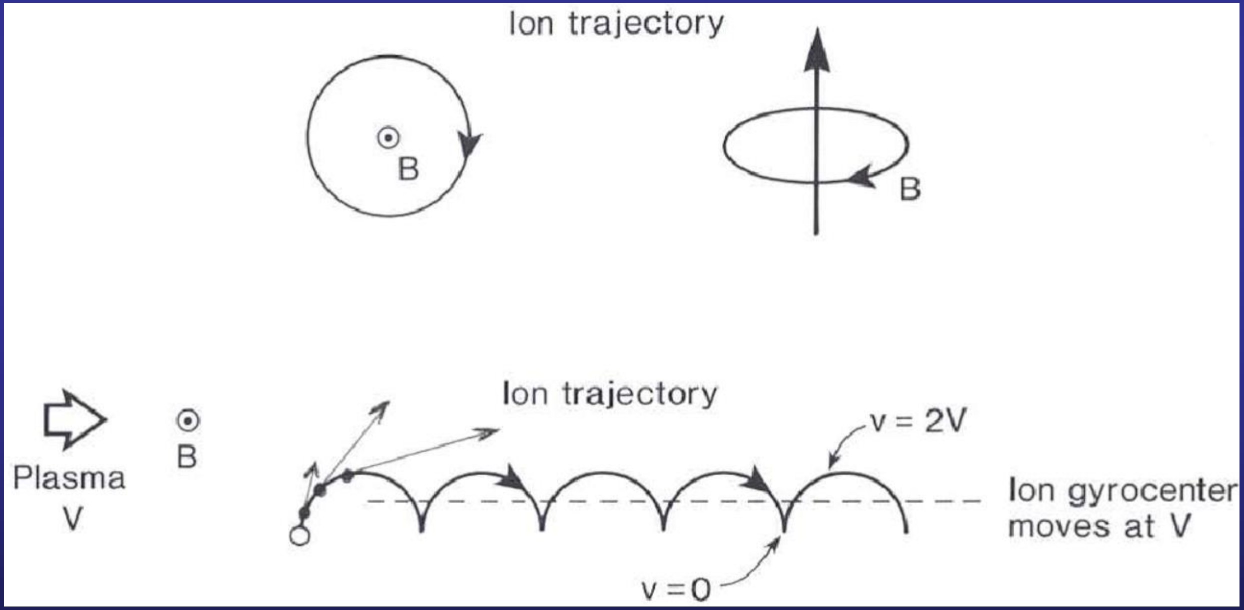

A.3: Plasma moments calculation

$$\mathbf{M}^k = \int f(\mathbf{v})(\mathbf{v})^k d^3\mathbf{v}$$

$$n = \int_{\mathbf{v}} f(\mathbf{v}) d^3\mathbf{v} = \int d\varphi \int d\vartheta \sin\vartheta \int dv v^2 f(v, \vartheta, \varphi)$$

$$n = 4\pi \int_{\mathbf{v}} f(\mathbf{v}) v^2 dv$$

$$J(E, \Omega, r) = \frac{v^2}{m} f(\mathbf{r},\mathbf{v}) = \frac{2E}{m^2} f(\mathbf{r},\mathbf{v})$$

A.3: Plasma moments calculation

$$\mathbf{M}^k = \int f(\mathbf{v})(\mathbf{v})^k d^3\mathbf{v}$$

$$G(E, \varphi, \vartheta)$$

$$c(E, \varphi, \vartheta)$$

$$J = \frac{c(E, \varphi, \vartheta)}{G(E, \varphi, \vartheta)\tau\Delta E}$$

$$n = \sum_{\varphi} \Delta\varphi \sum_{\vartheta} \Delta\vartheta \sin\vartheta \sum_{E} \frac{c(E, \varphi, \vartheta)}{G(E, \varphi, \vartheta)\tau v(E)}$$

A.3: Plasma moments calculation

$$n\mathbf{v} = \int_{\mathbf{v}} \mathbf{v} f(\mathbf{v}) d^3\mathbf{v}$$

$$\begin{aligned}
nv_x &= \int d\varphi \cos\varphi \int d\vartheta \sin^2\vartheta \int dE J(E,\vartheta,\varphi) \\
nv_y &= \int d\varphi \sin\varphi \int d\vartheta \sin^2\vartheta \int dE J(E,\vartheta,\varphi) \\
nv_z &= \int d\varphi \int d\vartheta \sin\vartheta \cos\vartheta \int dE J(E,\vartheta,\varphi)
\end{aligned}$$

A.3: Plasma moments calculation

$$\mathbf{P} = m \int_{\mathbf{V}} (v_i - v_k)(v_i - v_k) d^3\mathbf{v} = m[\mathbf{M}^2 - n v_i v_k]$$

$$\mathbf{M}^2 = \int_{\Omega} \int_{\mathbf{V}} v_i v_k f(\mathbf{v}) d\Omega d\mathbf{v}.$$

$$
\begin{aligned}
P_{xx} &= m \int d\varphi \cos^2\varphi \int d\vartheta \sin^3\vartheta \int dE v J(v,\vartheta,\varphi) - m v_x^2 n \\
P_{yy} &= m \int d\varphi \sin^2\varphi \int d\vartheta \sin^3\vartheta \int dE v J(v,\vartheta,\varphi) - m v_y^2 n \\
P_{zz} &= m \int d\varphi \int d\vartheta \sin\vartheta \cos^2\vartheta \int dE v J(v,\vartheta,\varphi) - m v_z^2 n
\end{aligned}
$$

A.3: Plasma moments calculation

$$P = \frac{P_{xx} + P_{yy} + P_{zz}}{3},$$

$$T = \frac{P}{2nK} \Rightarrow T[eV] = 3122 \frac{P[nPa]}{n[cm^{-3}]},$$

A.3: Plasma moments calculation

$$f(v) = C \cdot e^{-\frac{(v-\bar{v})^2}{v_t^2}}$$

$$C = \frac{n}{(\sqrt{\pi} v_t)^3}$$

$$v_t = \sqrt{\frac{2E_t}{m}}$$

$$f(E) = n \cdot \left(\frac{m}{\pi 2E_t}\right)^{3/2} \cdot e^{-\frac{E-2\sqrt{E\bar{E}}+\bar{E}}{E_t}}$$

$$\bar{E} = \frac{\int_E E \cdot f(E)}{\int_E f(E)}$$

$$\bar{f}(E)[\mathrm{s}^3/\mathrm{km}^6] = 0.86 \cdot 10^6 n \cdot \left(\frac{m}{E_t}\right)^{3/2} \cdot e^{-\frac{E-2\sqrt{E\bar{E}}+\bar{E}}{E_t}}$$

$$f(E) = \frac{J(E)m^3}{p^2} = \frac{J(E)m^2}{2E}$$

$$f(E) = \frac{m^2}{2G\tau} \frac{c(E)}{\Delta E \cdot E}$$

A.3: Parameters
Phase space density and diffusion equation

Phase space density

$$f_p = \frac{dN}{dx\,dy\,dz\,dp_x dp_y dp_z} = const$$

z is direction of particle motion

$$dz = v\,dt;\; dx\,dy = dA;\; dp_x dp_y dp_z = p^2 dp d\Omega_s$$

particle flux

$$j = \frac{dN}{dA\,dt\,d\Omega_s v\,dp}$$

$$f_p = \frac{j}{p^2} = const$$

radial diffusion :

$$\frac{\partial f_p}{\partial t} = L^2 \frac{\partial}{\partial L}\left(\frac{1}{L^2} D_{LL} \frac{\partial f_p}{\partial L}\right) + Q - S \qquad \text{often } D_{LL} = D_0 L^n$$

A.3: Parameters
Energetic Particle energy spectra

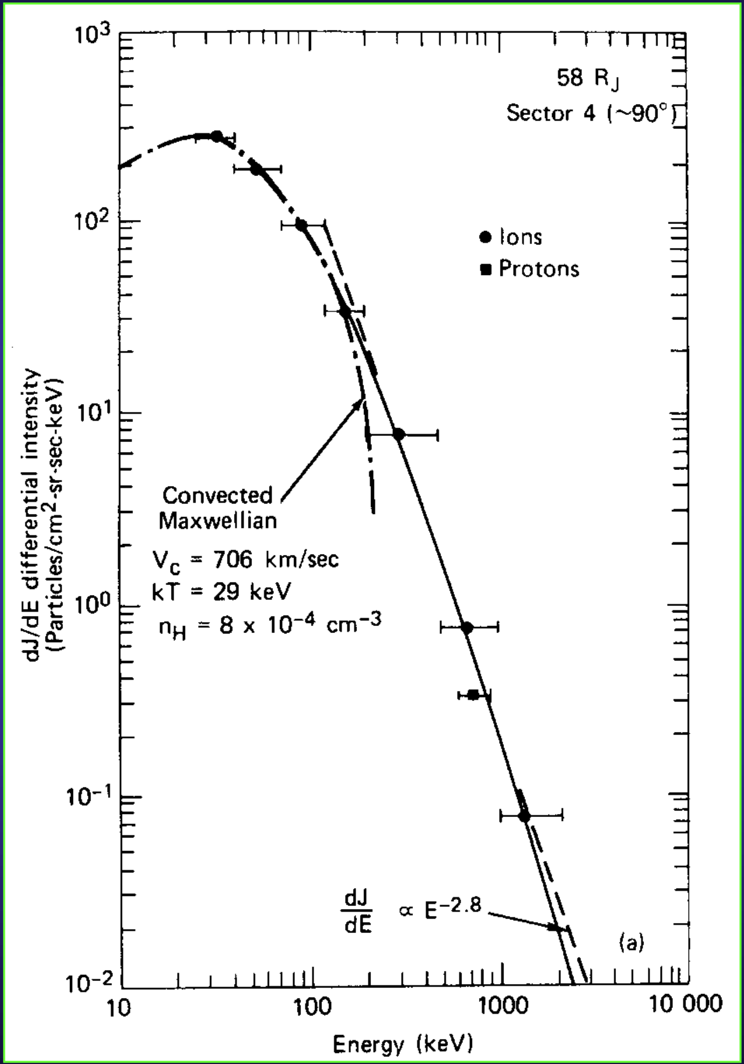

power law distribution:

$$I = I_0 \cdot \left(\frac{E}{E_0} \right)^{-\gamma}$$

slope γ is called spectral index

hard spectra: γ small

soft spectra: γ large

A.4: Instrumentation
Detector types

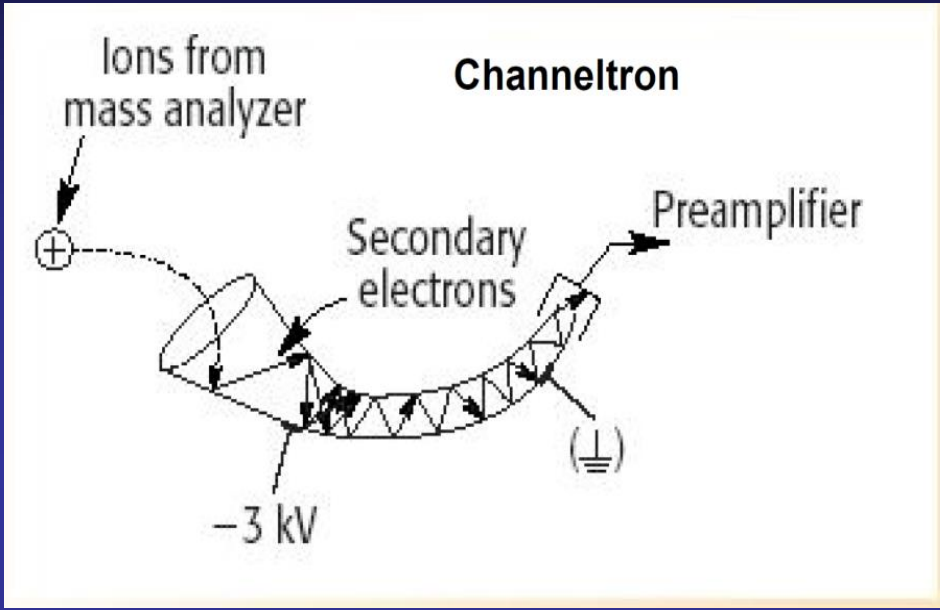

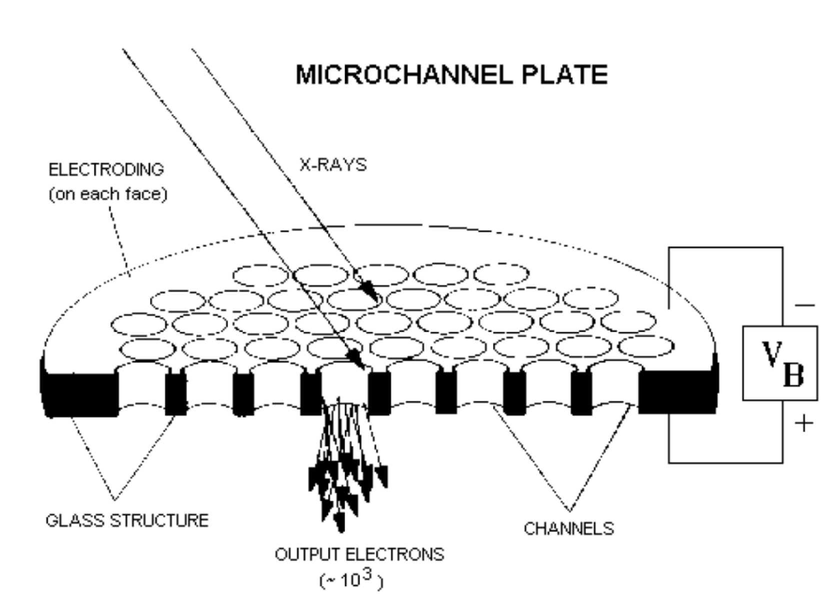

Channeltrons (CEMs)

Microchannel plates (MCPs)

are sensitive enough to detect electrons, ions and neutral atoms with an entrance energy of a few eV

A.4 Instrumentation
Instrument types

- Electrostatic spectrometers based on the deflection of particles in macroscopic electric and/or magnetic fields are limited for various reason to particle energies up to several 10 keV

- For energies > 10 keV Interaction with matter (or deflection in ‘atomic fields’) are used
  - Detector systems in telescope arrangements
  - The mass dependence of the specific energy-loss process is used in combination with different algorithms.

    Measured quantity:MZ^2.
  - Time-of-flight technique with solid-state detector systems.

    Measured quantity: MZ^2, EIM, and E,

    allowing the separation of mass M and energy E.

A.4 Instrumentation
Instrument types

3 processes are of importance for energetic particle spectroscopy

- specific energy loss (dE/dx) in matter
- secondary-electron emission (SEE) (mainly import for TOF measurements)
- pulse shape analysis (PHA) based on a waveform analysis of the signal a particle leaves in a SSD (not of great practical importance low resolution)

A.4: Instrumentation
dE/dx vs. E measurements principle

Energetic particles traveling through matter lose energy continuously by Coulomb interaction with electrons and nuclei in the absorbing material. The amount of energy lost per unit path length is referred to as the electronic and nuclear specific energy loss *(dE/dx)e*, and *(dE/dx)n*, respectively. The energy loss due to nuclei collisions becomes significant only for particle energies below a few keV/nucleon, leaving *(dE/dx)e* in the energy range of interest as the dominant process. For particles with sufficiently large velocities the electronic energy loss is adequately described by the equation

$$-(\mathrm{d}E/\mathrm{d}x)_\mathrm{e} = k_1(MZ^2/E_0)f(E, k_2).$$

Here *M, Z* and *Eo* denote the mass, charge and energy of the particle. The parameters ***k1*** and *k**2*** depend only on the target material. The function *f(E,k2)* varies only slowly with particle energy *E.*

A.4: Instrumentation
dE/dx vs. E measurements principle

How to extract mass information from a (dE/dx) and *E* measurement?

The general concept of such an instrument is to arrange two suitable detectors, such as proportional counters or solid-state detectors, in a telescope configuration.

If the thickness ΔX of the front element is chosen to be small compared to the range of the incident particle the energy loss ΔE is approximately equal to (dE/dx)ΔX.

The back detector of the telescope must be thick enough to absorb the entire residual energy E.

The ΔE and *E* signal provided by the telescope can then be used to determine the incident particle energy E*o (Eo= E* +ΔE) and to establish mass information by applying an appropriate algorithm or particle identifier function to the signal amplitudes.

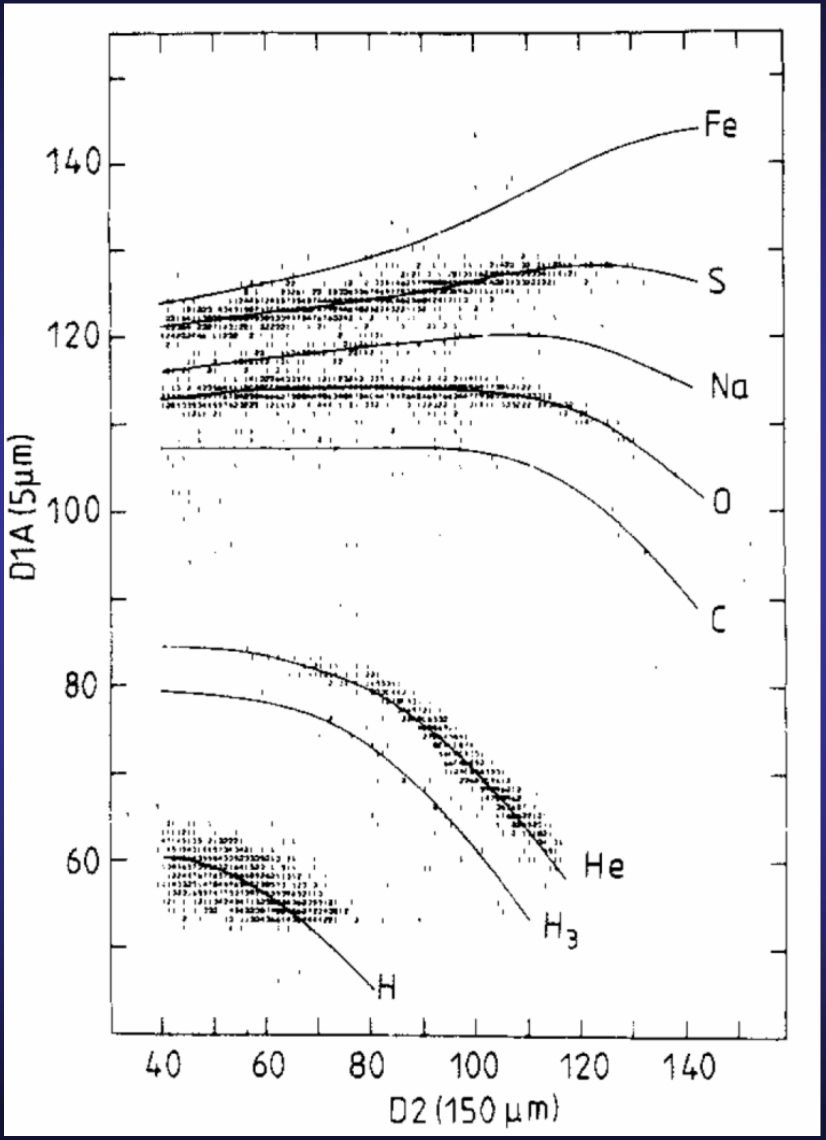

A.4 Instrumentation
Electrostaic analyzer ESA concept

- Collimator: (mechanical) device to limit the incoming particle beam to a small spatial opening angle and simultaneously provides a large aperture surface
- Analyzer: filters particles with pre-selected values of the particle parameters out of the beam for further analysis
- Detector: counts particles (eventually with energy determination)
- Electronics: includes power supplies, analog electronics to amplify the detector signal and to transform them for further analysis, DPU (interface to s/c and control unit)

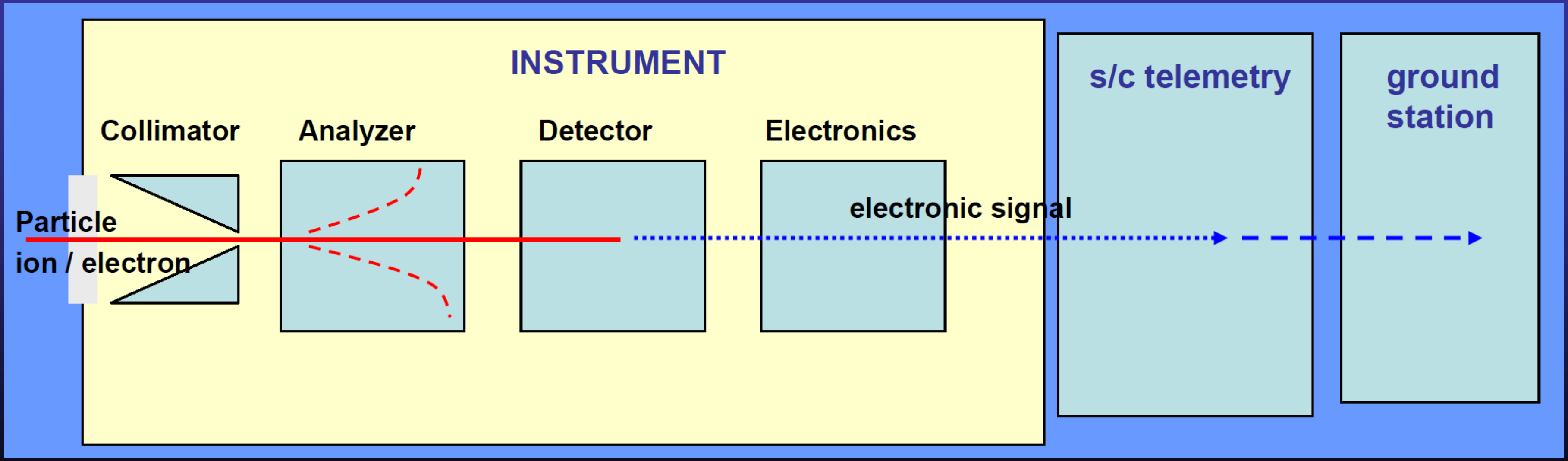

A.4 Instrumentation
Electrostatic analyzer ESA

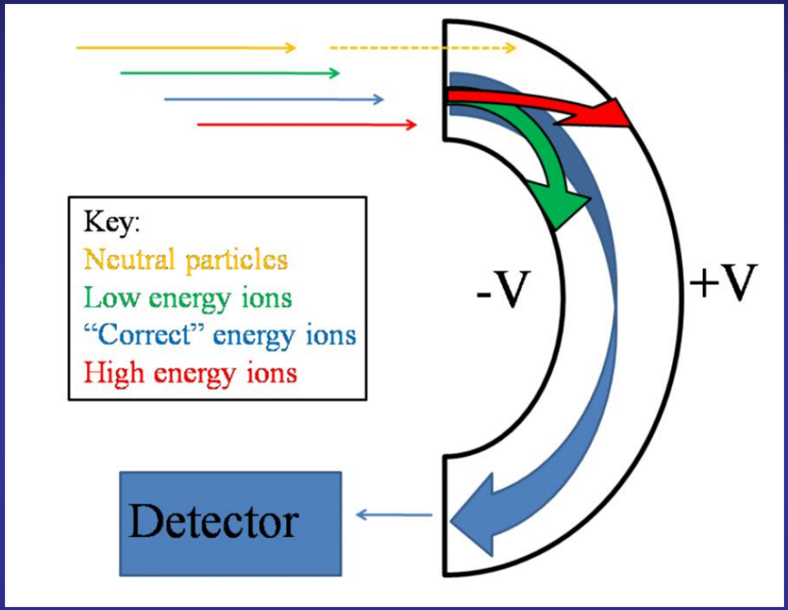

uses an electric field between two curved plates to guide the flight path of a charged particle around a bend to a detector.

The particle orbit through the curved plate analyzer is given by the force balance between the electric field force and the centripetal force.

The electric field E exerts a force qE on the particle that causes it to move in a great circle with radius r equal to mv2/qE.

particles pass if their energy/charge (E/q) fits.

The flux of plasma that enters the instrument is determined by the size of the aperture, A. The size of the detector, the voltage range and the polarity affects the energy and species detected.

Electrostatic analyzer in space

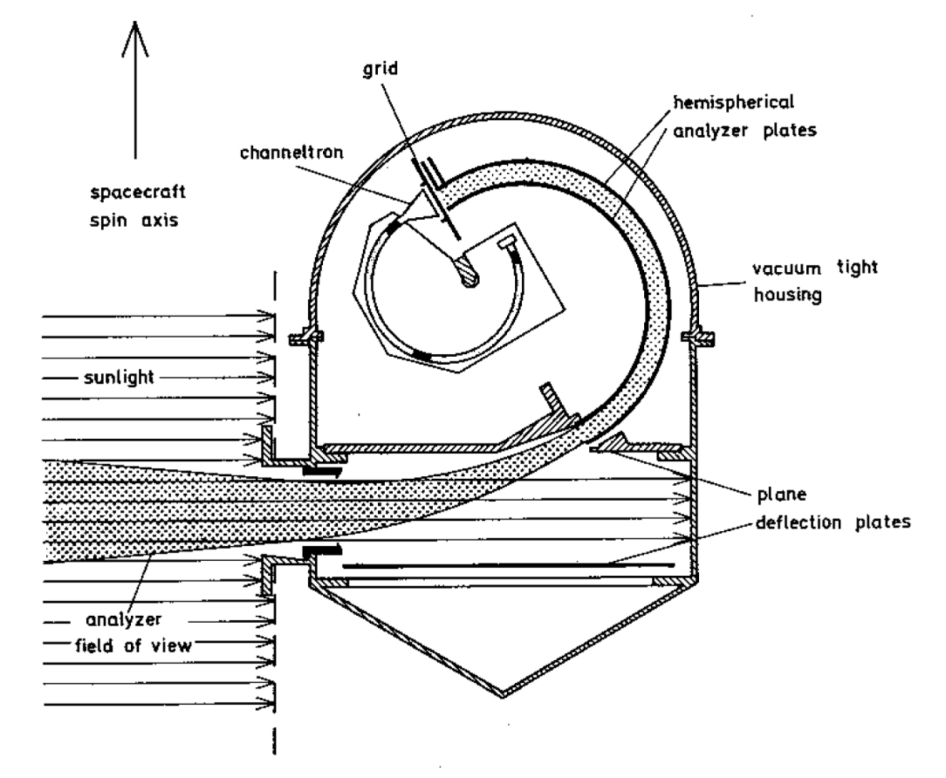

Scheme of the Helios E1 electron instrument (I2), invented in 1974 by H. Rosenbauer (later director at MPS).
The trick: no photo electron could ever make it to the detector!

A.4 Instrumentation
ESA Plasma composition measurements

The plasma composition is often quite variable and is an important diagnostic for the origin of that plasma.
The passage of an interplanetary coronal mass ejection (ICME). The counts as a function of energy per charge are shown for this interval.

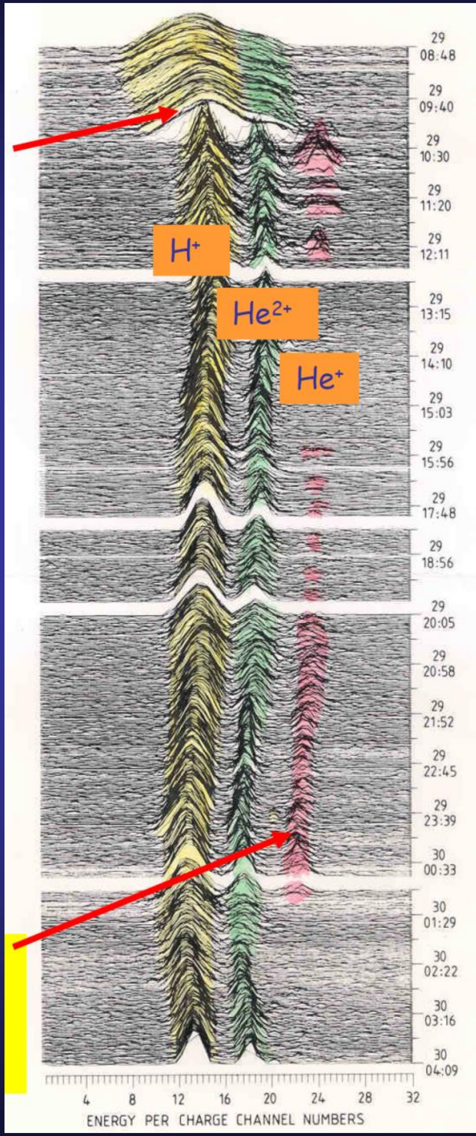

Discovery of singly ionized Helium ions in the driver gas following an interplanetary shock wave by **Helios 1** in January 1977: remnants of cold prominence material.

A.4 Instrumentation
Different types of ESAs

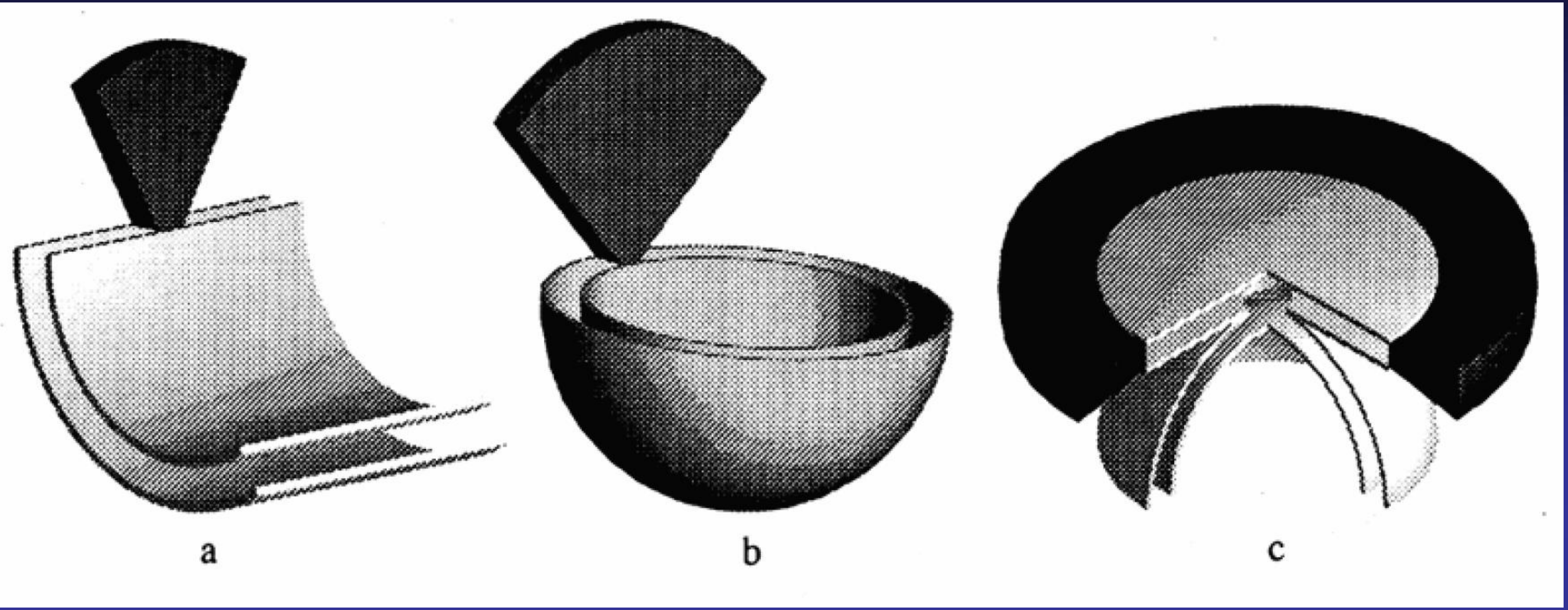

Funsten and McComas (AGU Monograph 1998)

On the left is a pair of cylindrical plates. In the middle are spherical plates and on the right is a so-called *top hat* design leading into a pair of spherical plates.

The *top hat analyzer* views a full 360 degrees in azimuth with a narrow fan in the orthogonal direction.

On a spinning spacecraft the field of view covers the complete sky.

On non-spinning spacecraft the FOV is extended by scanning platforms or electric deflection at sensor entrance.

A.4 Instrumentation
Plasma composition measurements with ESA

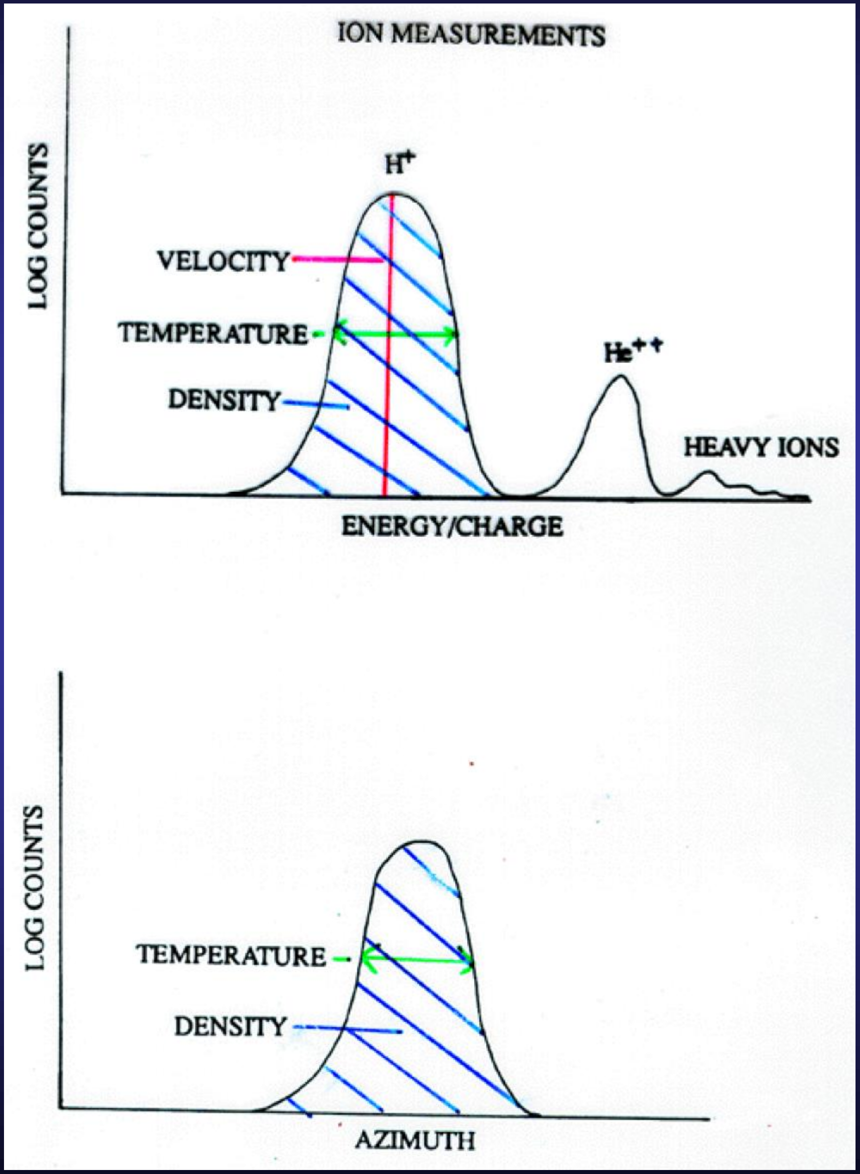

If ions move at the same velocity (as for example in the solar wind) an electrostatic analyzer is sufficient to:

1. separate ion species

    determine density, velocity and temperature of the distribution.

The maximum energy resolution achieved so far in space is 0.14% (Cassini CAPS IBS) sufficient to do isotopic analysis.

MAX-PLANCK-GESELLSCHAFT

Max-Planck-Institut für Sonnensystemforschung

A.4 Instrumentation ESA + magnetic deflection Example Mars Express ASPERA-IMA

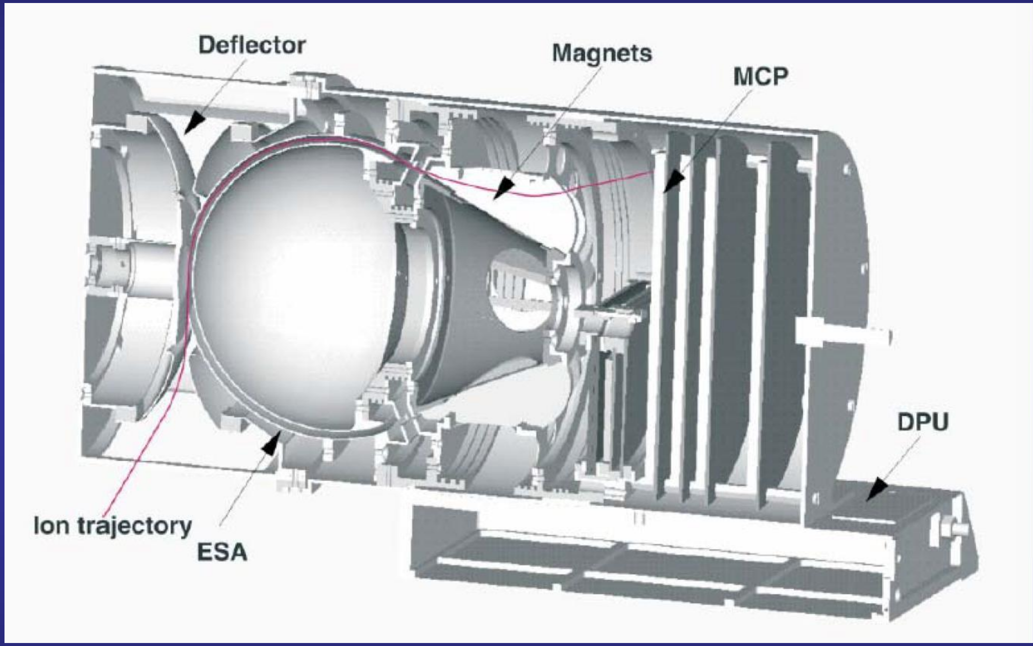

Parameter	*IMA*
Particles to be measured	ions
Energy range, keV per charge	0.01 - 30
Energy resolution, ΔE/E	0.07
Mass resolution	m/q = 1, 2, 4, 8, 16, >20
Intrinsic field of view	90 x 360°
Angular resolution (FWHM)	4.5 x 22.5°
G-factor / pixel, cm^2 sr	3.5×10^{-4}
Efficiency, ε, %	inc. in G
Time resolution (full 3D), s	32
Mass, kg	2.2
Power, W	3.5

Combinations of electrostatic and magnetic sector fields can be used for a determination of the mass-per-charge *(M / Q)* ratio of ions by combining the ***(E /*** *Q)* information from the deflection in an electrostatic analyser with the momentum-per-charge ***(P/****Q)* ratio obtained from a gyroradius measurement in a magnetic field.

A.4 Instrumenation
TOF-principle

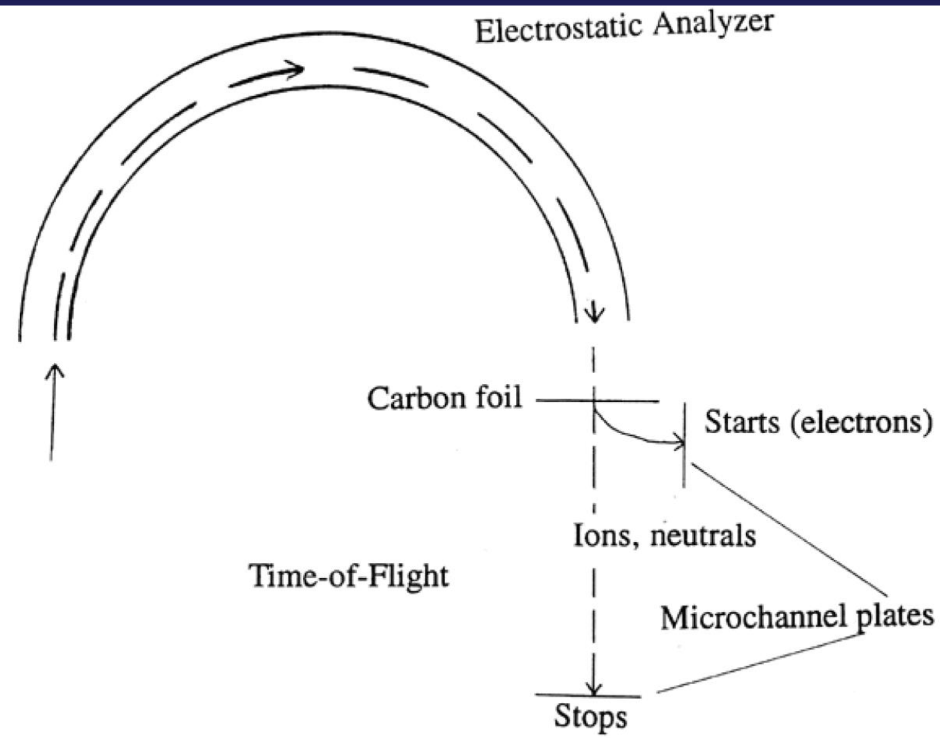

Major factor limiting M/Q resolution in traditional Time-of-Flight Plasma Instrument: Energy and angle straggling in carbon foils.

A simple time of flight analyzer When the ion leaves the analyzer section it passes through a very thin carbon film. This passage knocks out an electron that is captured by a positively charged plate and triggers a start pulse. When the ion reaches a stop plate another pulse is generated and the time between the pulses is the time of flight. The energy loss and angular spreading caused by the passage through the foil degrades the M/Q resolution here.

A.4 Instrumentation
Time-of-flight instrument

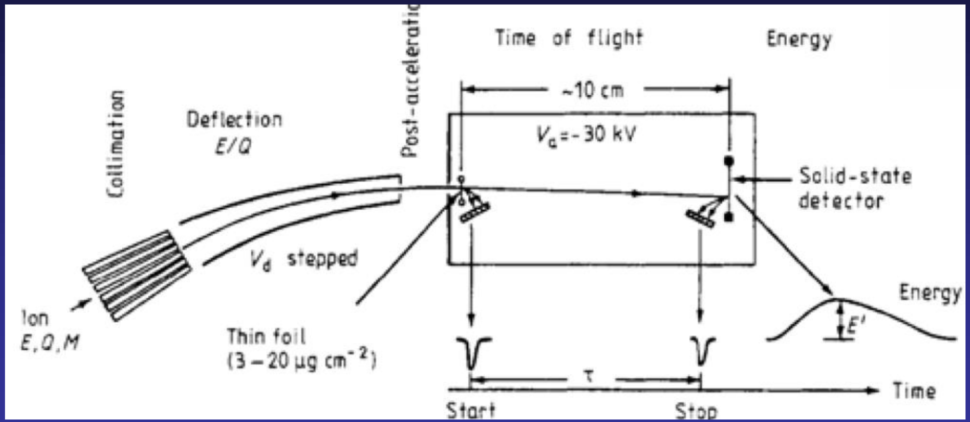

$$(M/Q) = 2[V_a + (E_0/Q)](d/T)^{-2}$$

$$M = 2(E\alpha)(d/T)^{-2}$$

$$Q = M(M/Q)^{-1}$$

$$E_0 = Q(E_0/Q).$$

parameter α accounts for energy losses in the carbon foil and in the entrance window of the detector, as well as for non-ionising collisions (nuclear defect) in the detector bulk material

ESA selects ions according to E0/Q according to deflection voltage Vd
exiting ions are post-accelerated by potential drop Va
accelerated ions enter into the TOF – E system
• ions enter through a thin Carbon foil
• secondary electrons emitted from the foil and detected by an MCP provide start time
• stop time is provided by secondary electrons emitted from the surface of a Solid State Detector
• SSD measures the residual energy E (based on E - ΔE technique, or PHA)

A.4 Instrumenation
Bepi Colombo SERENA/MSA

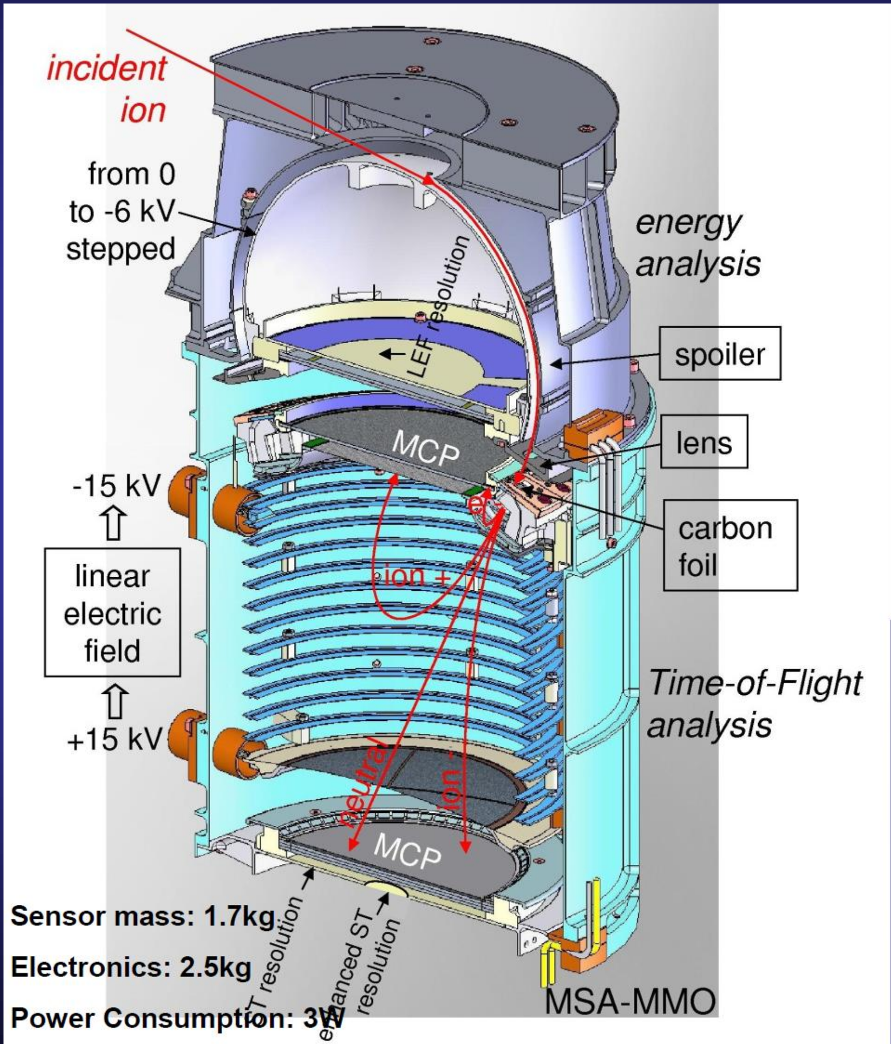

Sensor mass: 1.7kg

Electronics: 2.5kg

Power Consumption: 3W

- FOV : 8° x 260° (after closing due to mast)
- angular resolution (max) : 8° x 11.25°
- energy range : 5 eV/q – 40 keV/q
- energy steps : 32 or 64 steps (nominal step duration : 3.9 ms)
- energy resolution : 10 %
- analyzer constant : 7.1
- inner deflector radius : 57.9 mm
- outer deflector radius : 61.9 mm
- deflection angle : 110°
- mass range : 1-60 amu
- mass resolution : m/Δm = 40 for energies < 15 keV/q (nominal)
  m/Δm = 10 for energies > 15 keV/q
- time resolution : 3D distribution in 4 s (32 energies)
  3D distributions in 8 s (64 energies)
- G-factor : 1.9×10^{-3} cm2 sr keV/keV (nominal)
  1.9×10^{-7} cm2 sr keV/keV (for solar wind ions)

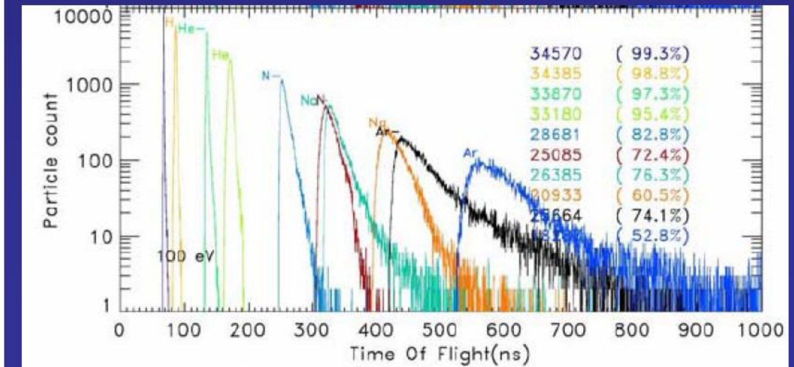

Figure 2.3-7 Model TOF spectra for various species on the ST detector.

A.4 Instrumentation
ESA+TOF without C-foil
BepiColombo SERENA/PICAM

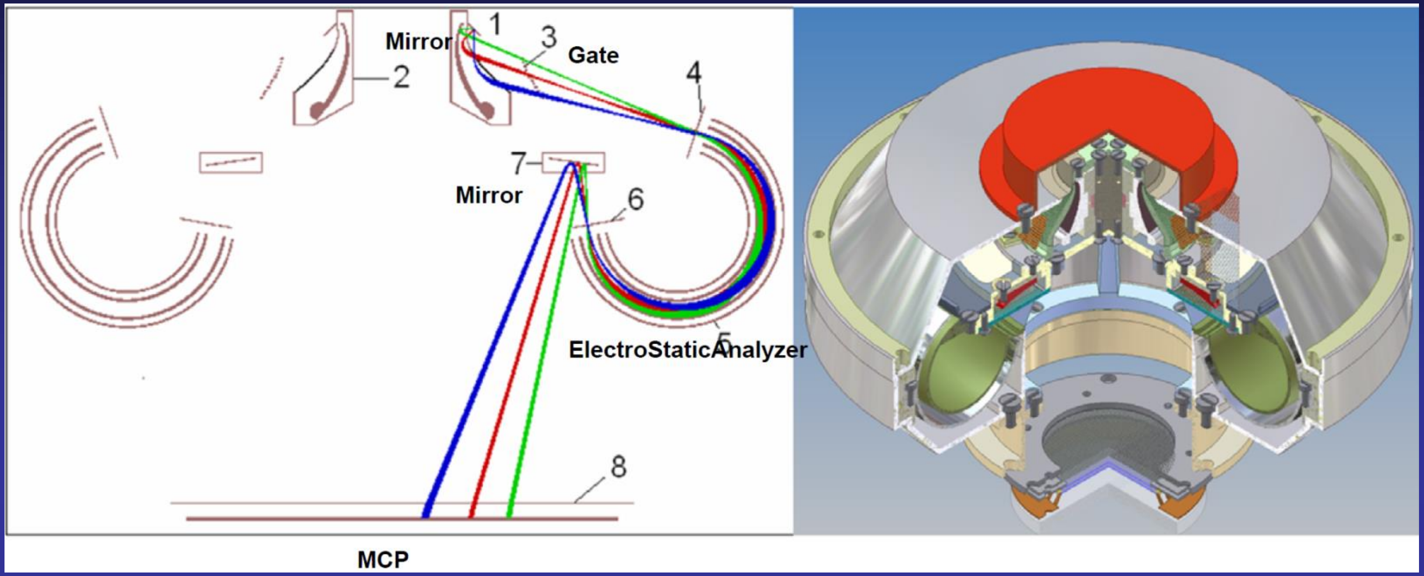

Ions are reflected by electrostatic mirrors such that an image of the particle distribution is projected onto the MCP.
In addition TOF can be measured by switching flow On and Off using an electric gate.

A.4: Instrumentation
Things to worry about when designing a particle detector

- accommodation on the spacecraft
- limited power available for the instrument
- the mass and volume available
- stabilization of the spacecraft (spinning / non-spinning)
- electrostatic cleanliness of the spacecraft
- telemetry rate to transmit all this information back to Earth
- knowledge about plasma environment to be encountered.. Will there be a cold beam like the solar wind or a hot plasma such as the Earth's plasma sheet?
- will there be an intense radiation belt (false counts, decrease the life of the instrument)
- what is the resolution required in time, angle, energy and mass per charge to achieve to meet the scientific objectives?
- what is the range required in energy and density to measure the plasmas encountered

A.4 Instrumentation
How to measure neutrals?

- *step 1*: prevent ions and electrons to enter the instrument
- →electric and magnetic deflection systems
- *step 2*: reduce UV and EUV
- →foils, grates
- *step 3*: convert neutral particle into ion
- →ionizing foils, grazing incidence on surfaces
- *step 4*: perform spectral, mass analysis
- →E + B fields, TOF system, E-PHA
- *step 5*: perform imaging
- →direction-sensitive detection (MCP, SSD)
- *conserve velocity and directional information* and *combine it with a high geometric factor !*

ENA principle

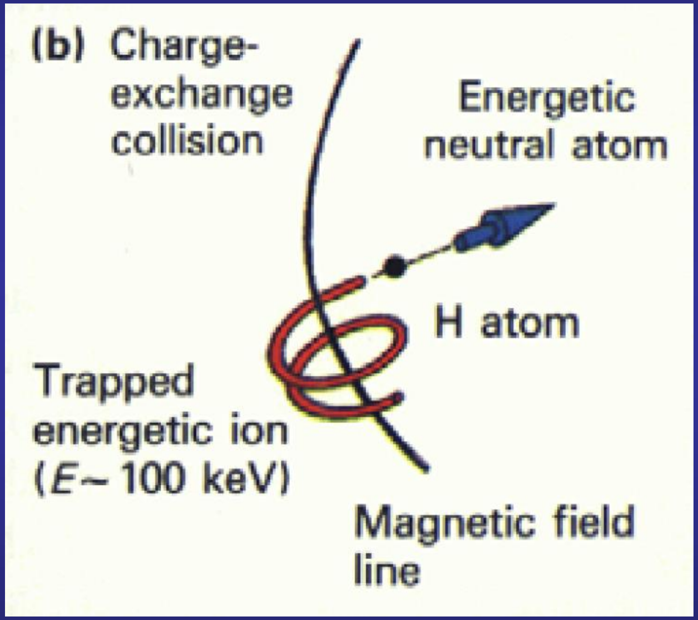

The co-existence of an energetic charged particle population (solar wind, magnetospheric plasma) and a planetary neutral gas leads to interaction, e.g., through charge-exchange:

A^+(energetic) + P(cold) ⇒ A(energetic) + P^+(cold)

Little exchange of momentum → conserve velocity

ENA are not influenced by E- and B-fields; they travel on straight ballistic path like a photon

Directional detection of ENAs yields a global image of the interaction and allows to deduce properties of the source populations.

ENA production mechanism in space plasmas

Charge - exchange reaction with atmospheric / exospheric gases

Sputtering of planetary atmospheres

Backscattering from the planetary atmospheres (ENA albedo)

Sputtering from planetary surfaces

Ion neutralization / sputtering on dust particles

Recombination (CMI)

A.4 Instrumentation
Neutral particle detectors

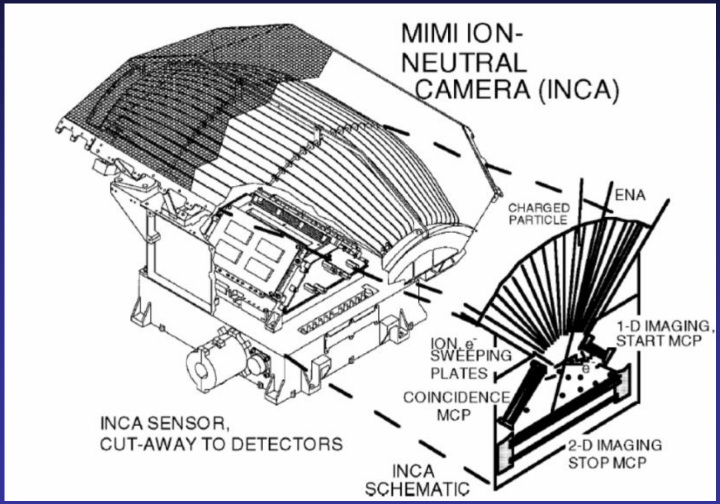

MIMI/INCA sensor on Cassini measures high-energy neutrals

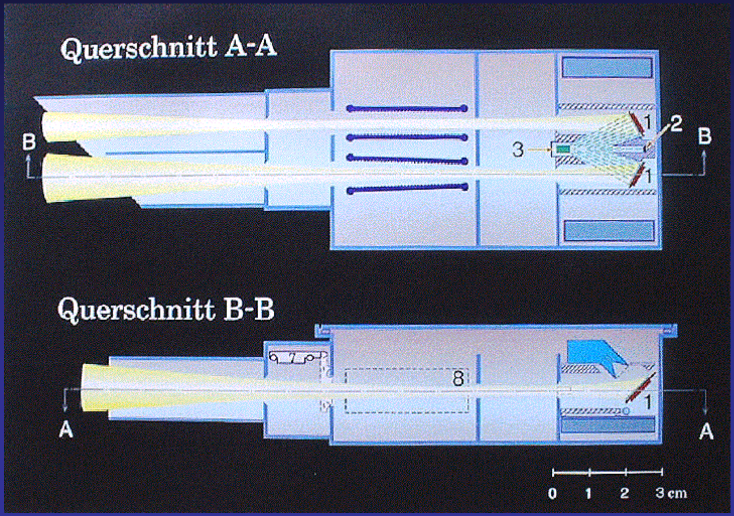

GAS instrument on Ulysses measured cold neutral gas

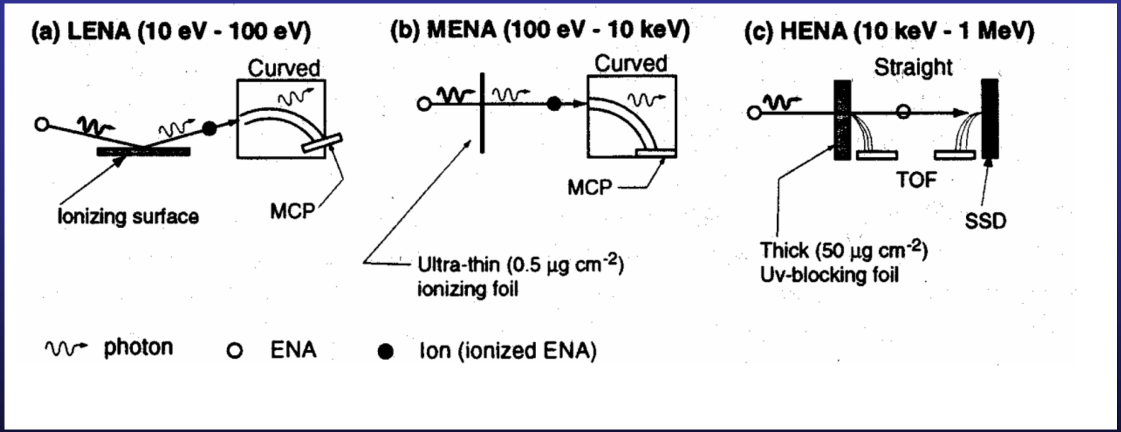

Grazing incidence principle on Bepi Colombo

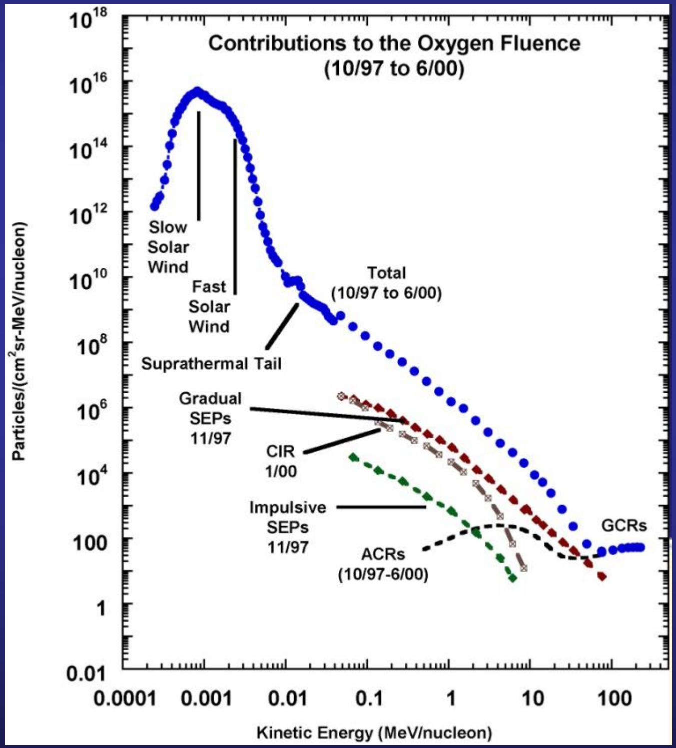
Contributions to the Oxygen Fluence
(10/97 to 6/00)
Slow Solar Wind
Fast Solar Wind
Suprathermal Tail
Total (10/97 to 6/00)
Gradual SEPs 11/97
CIR 1/00
Impulsive SEPs 11/97
ACRs (10/97-6/00)
GCRs
Particles/(cm²sr-MeV/nucleon)
Kinetic Energy (MeV/nucleon)

B. Energetic particles from the Sun

1. Coronal mass ejections
2. Flares

will follow

C. Energetic particles at shocks

1. Acceleration at interplanetary shocks
2. Corotating interaction regions (CIR)
3. Particles from the heliospheric termination shock
4. Acceleration at planetary bow shocks

C. Energetic particles in interplanetry space

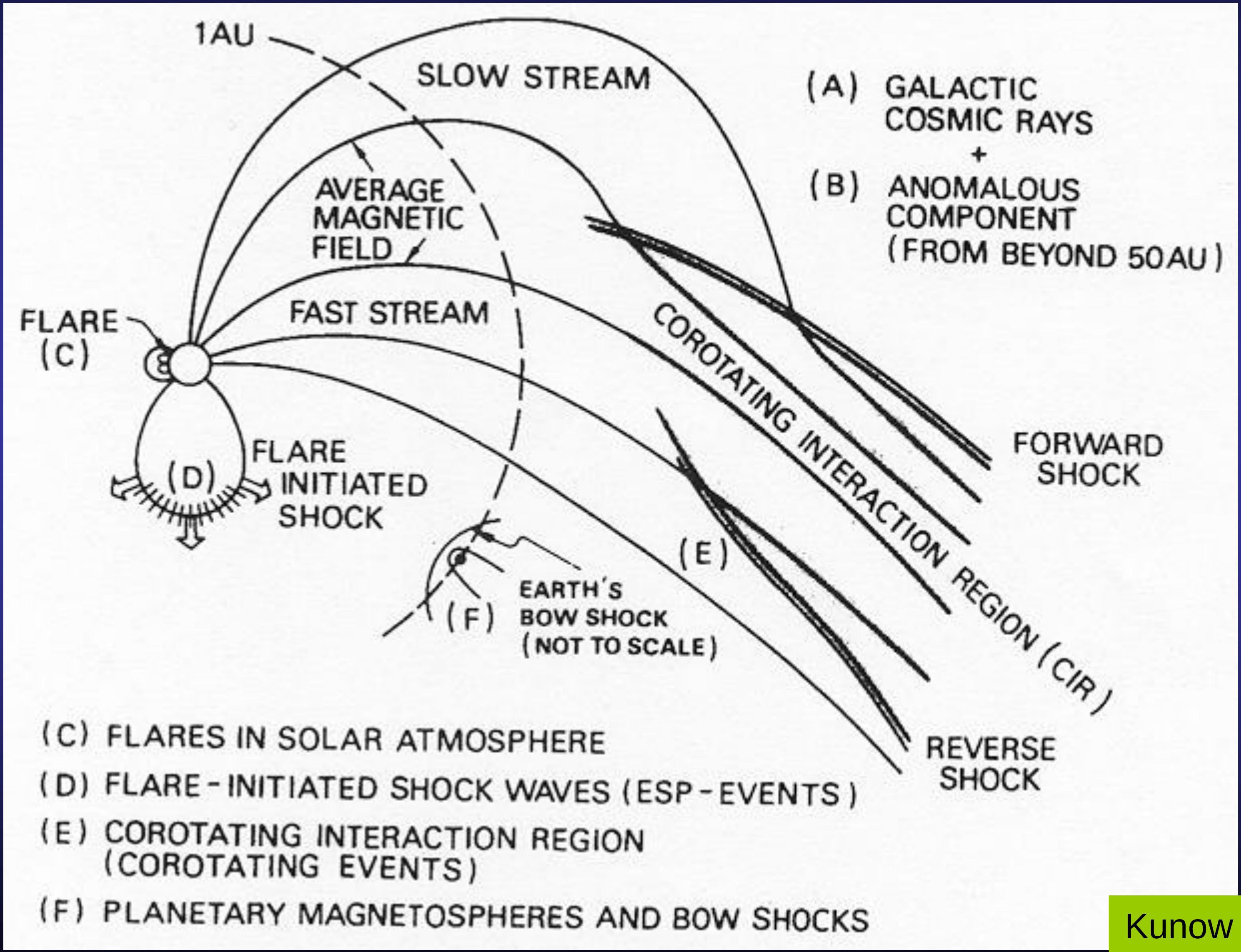

Kunow et al., 1991

Energy spectra of heliospheric ion populations

- How are they accelerated?
- What is their composition?
- How do they propagate?
- What are the source spectra?

Energies: 1 keV - 100 MeV

Sources: Mainly shock acceleration at flares/CMEs and CIRs

Gloeckler, Adv. Space. Res. **4**, 127, 1984

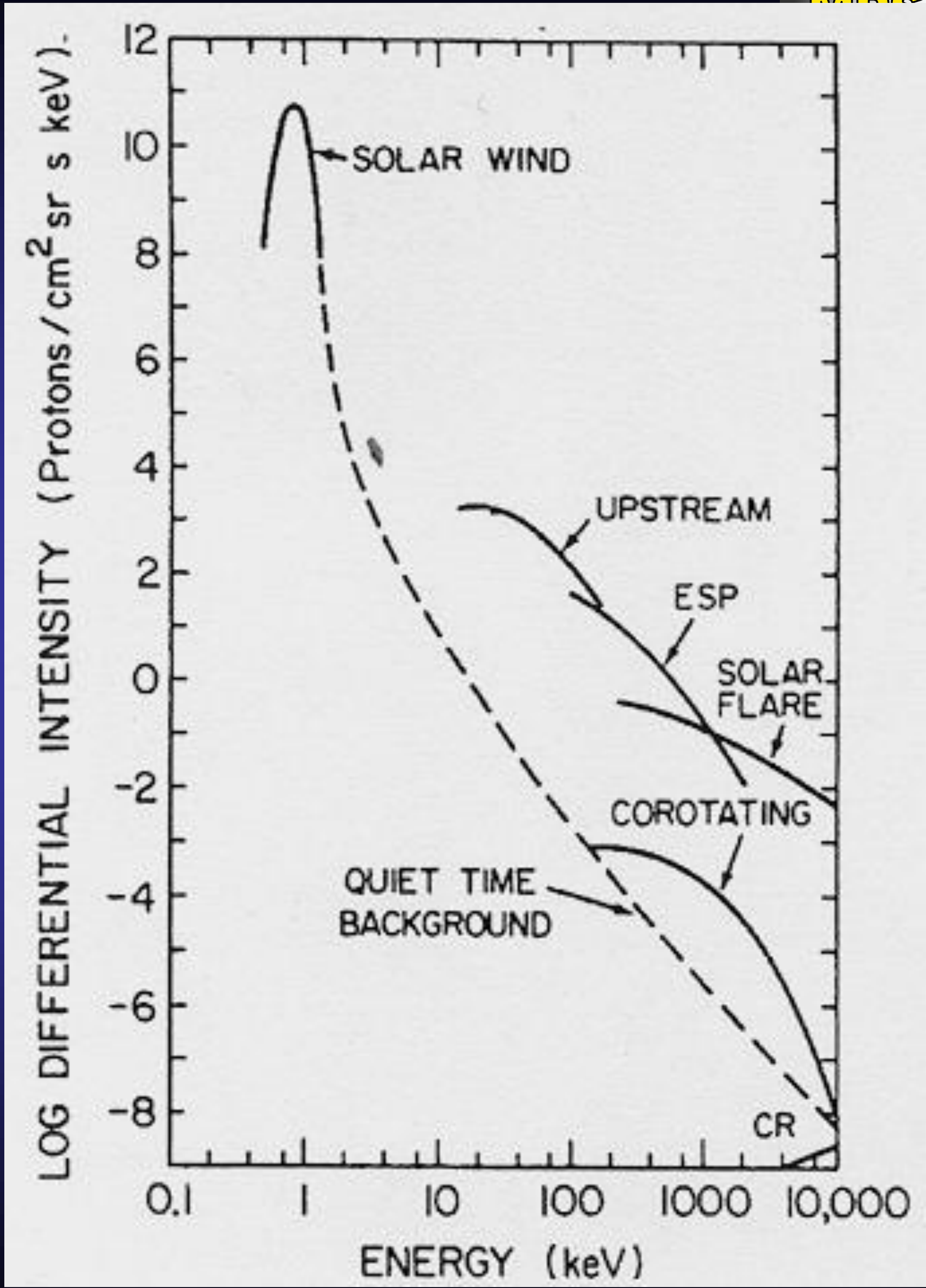

Structure of the heliosphere

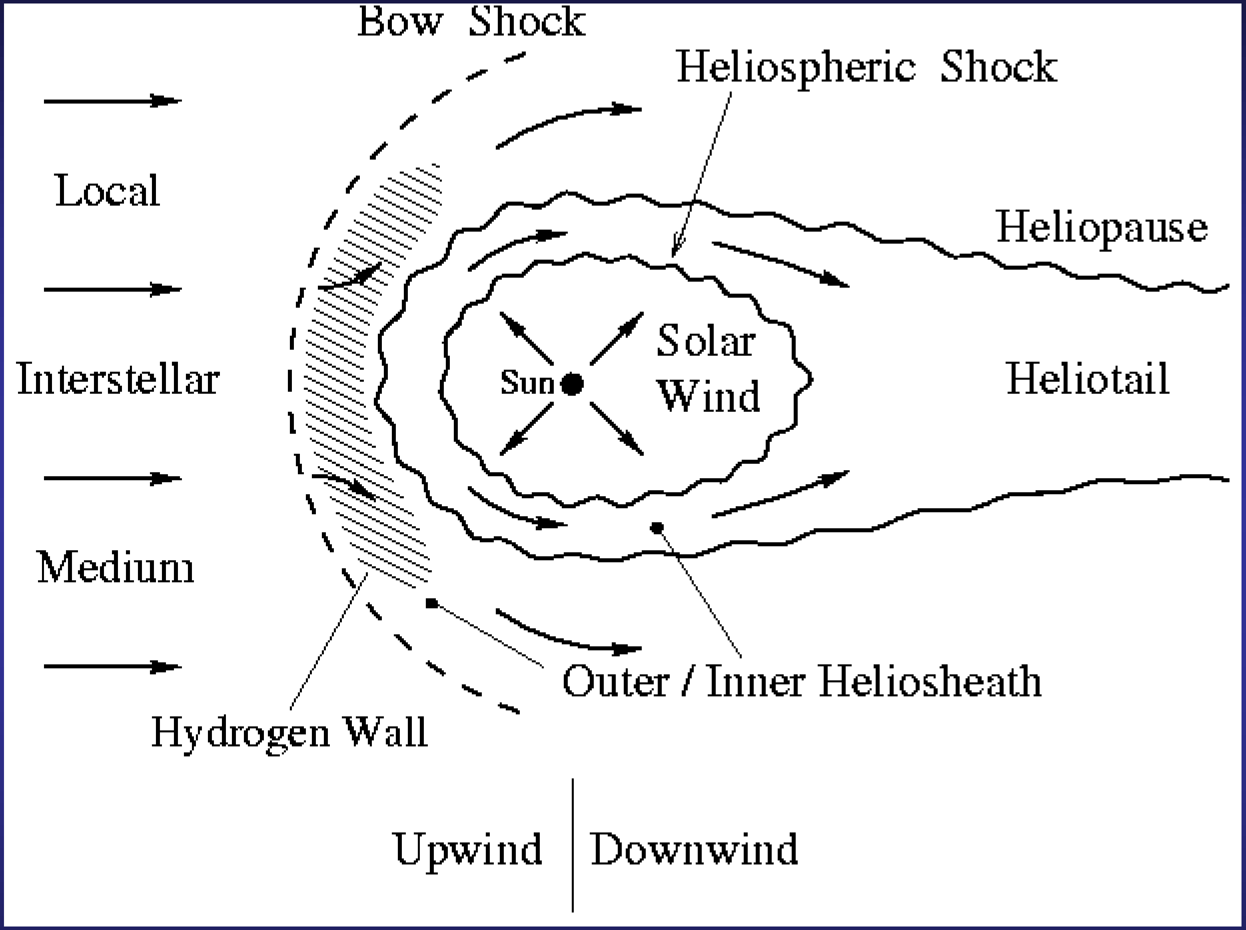

- Basic plasma motions in the restframe of the Sun
- Principal surfaces (wavy lines indicate disturbances)

C.4 Earth's bow shock

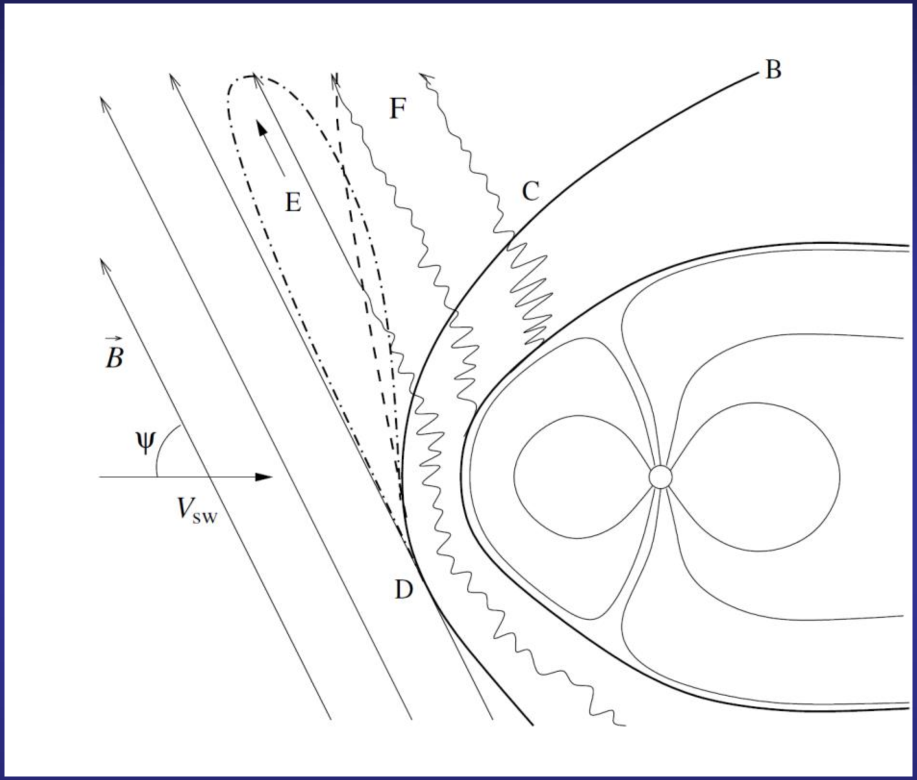

Fast-mode shock
 Shape ~ hyperboloid
Region between the shock (B) and the magnetopause (A) called *magnetosheath*
 In regions with *n perp B*1 (D), flow and field nearly laminar
 In regions with *n parallel B*1 (C), flow and fleld very turbulent
→ foreshock region with reflected particles (F: ions, E: electrons) and turbulent fields (generated by streaming instabilities)

more to come

D. Energetic particles from interstellar space

1. Galactic cosmic rays
2. insterstellar neutrals

E. Energetic particles in planetary magnetospheres

1. Radiation belts, Synchrotron radio emissions
2. Magnetodisc and magnetotail regions
3. lobes and polar magnetosphere / aurorae
4. Energetic particles measurements as a useful tool to study plasma processes in magnetospheres and moon-magnetosphere interaction

E. Energetic particles at Jupiter (Galileo/EPD)

Saturn (Cassini/MIMI)

Max-Planck-Institut für Sonnensystemforschung

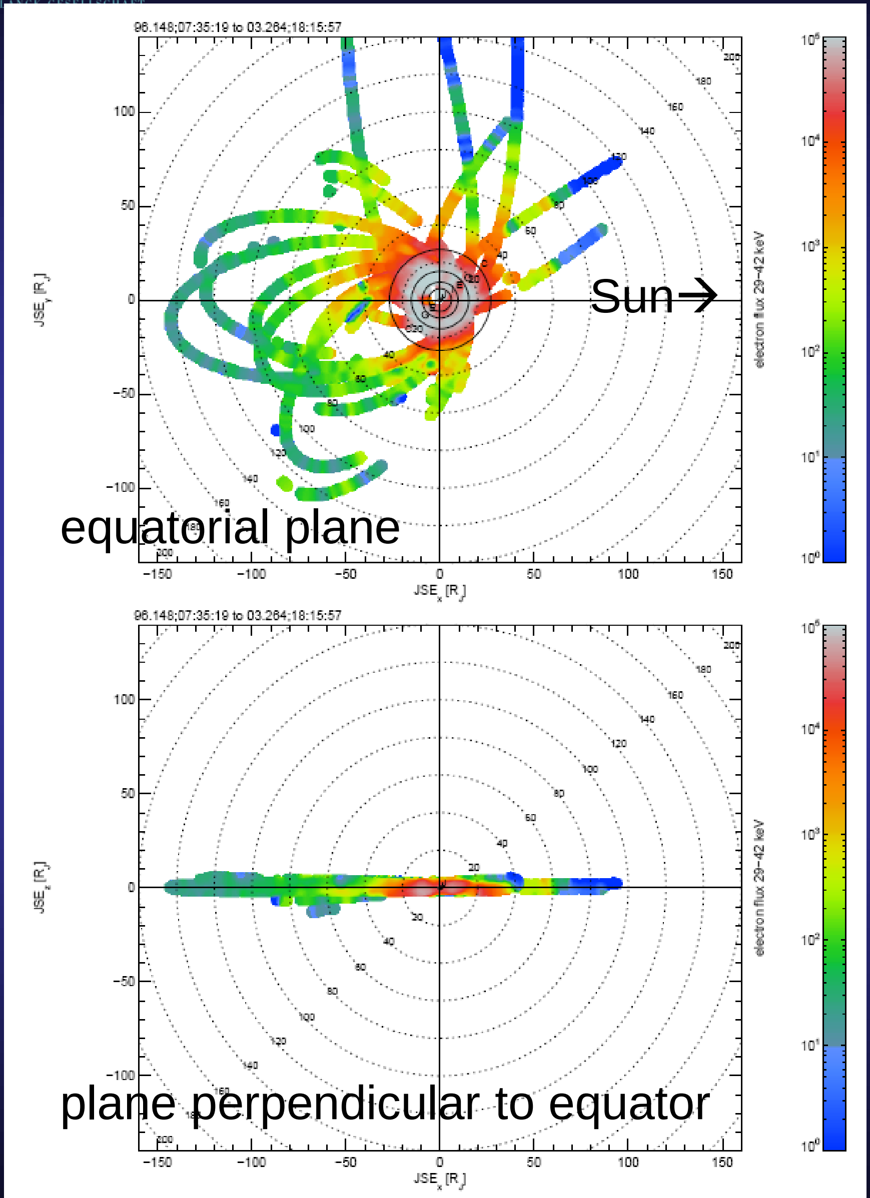

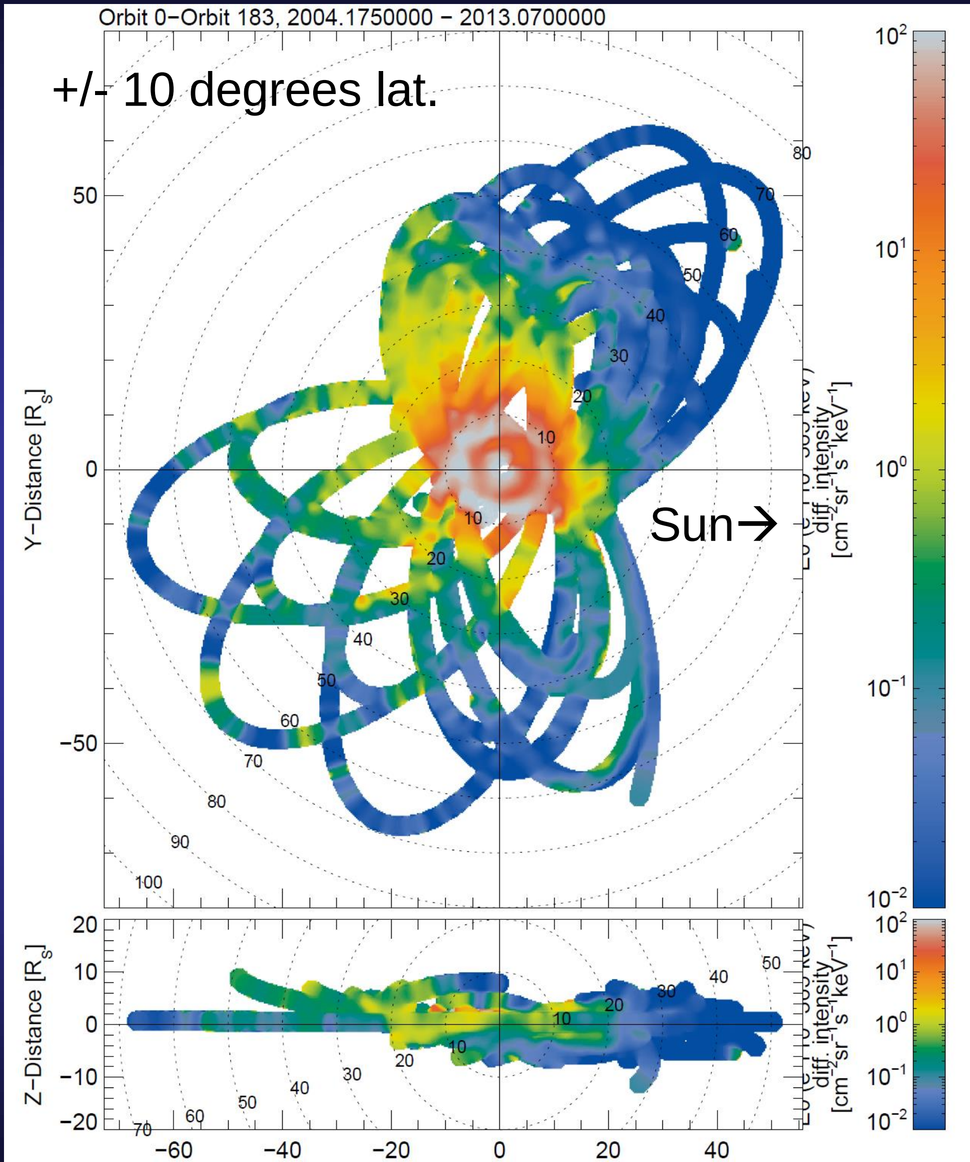

E.1. Radiation belts
Discovery at Earth

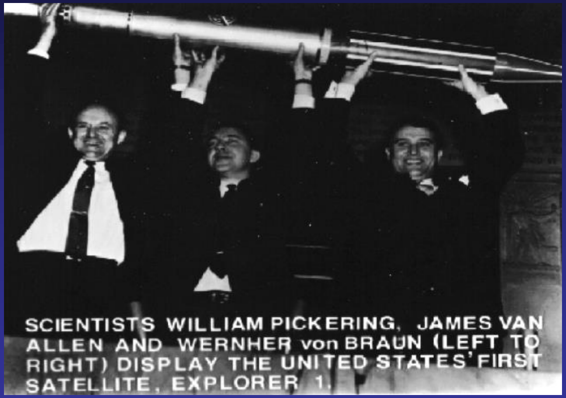

Explorer 1 (Jan 31, 1958) carried a Geiger Counter to study the latitudinal distribution of low-energy cosmic ray it failed in that instead it discovered Earth's radiation belts (by saturation of counters)
This was confirmed by Sputnik 3 in the same year.

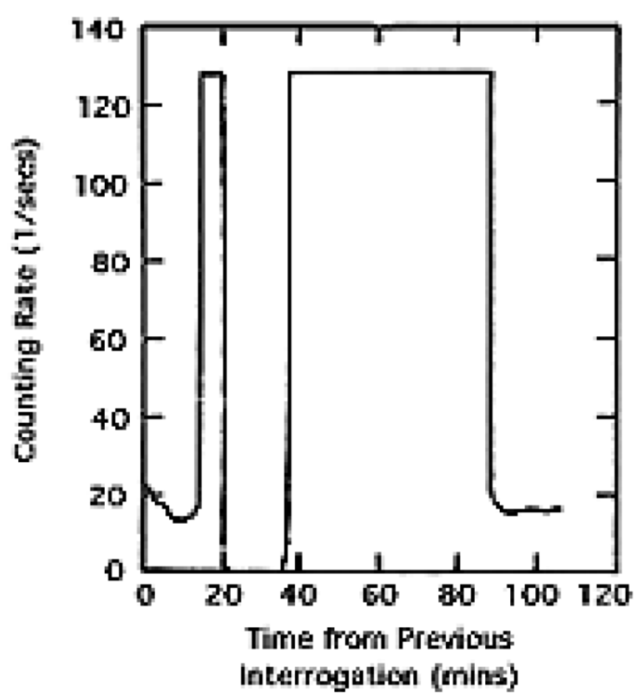

tape recorder read-out from Explorer 3

Jupiter's radiation belts -
a very harsh environment !!

DIVINE + GIRE JOVIAN RADIATION MODELS

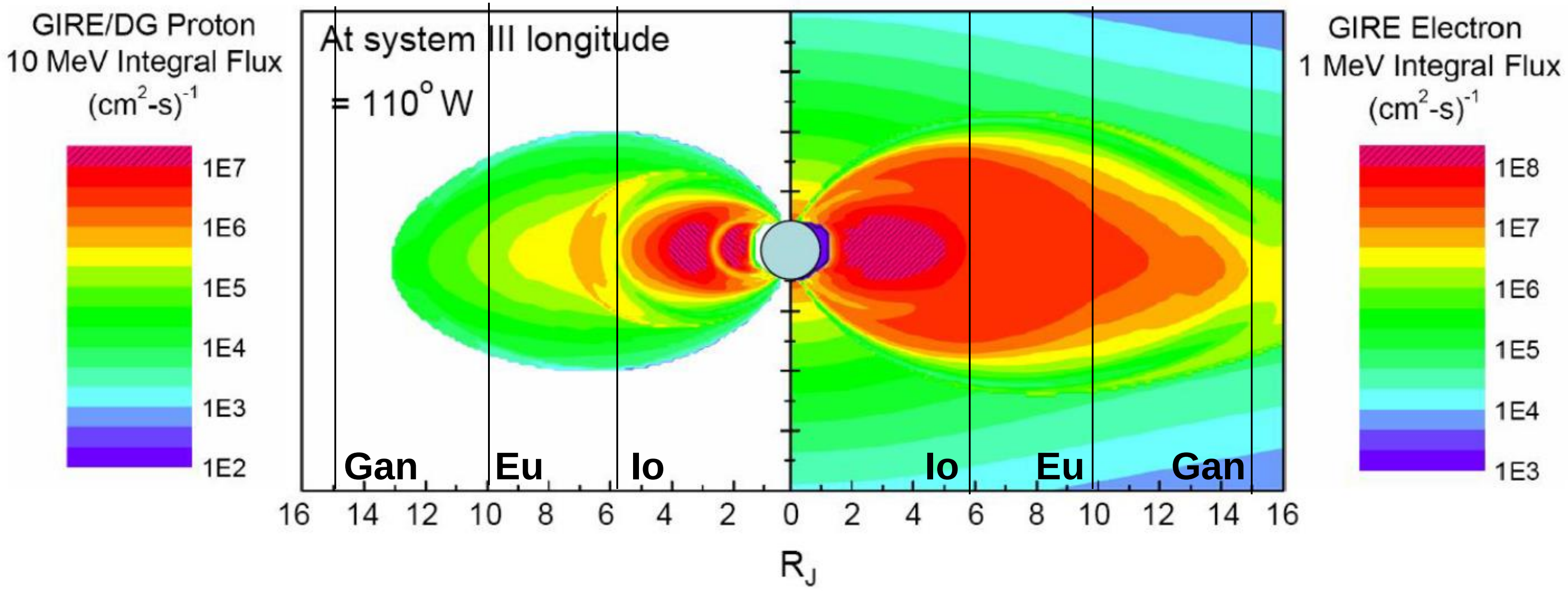

Contour plots of $\geq$1 MeV electron and $\geq$10 MeV proton integral fluxes at Jupiter. Coordinate system used is jovi-centric. Models are based on Divine/GIRE models. Meridian is for System III 110° W.

E.1 Saturn's radiation belts

Roussos et al., 2008
Gombosi et al., 2009

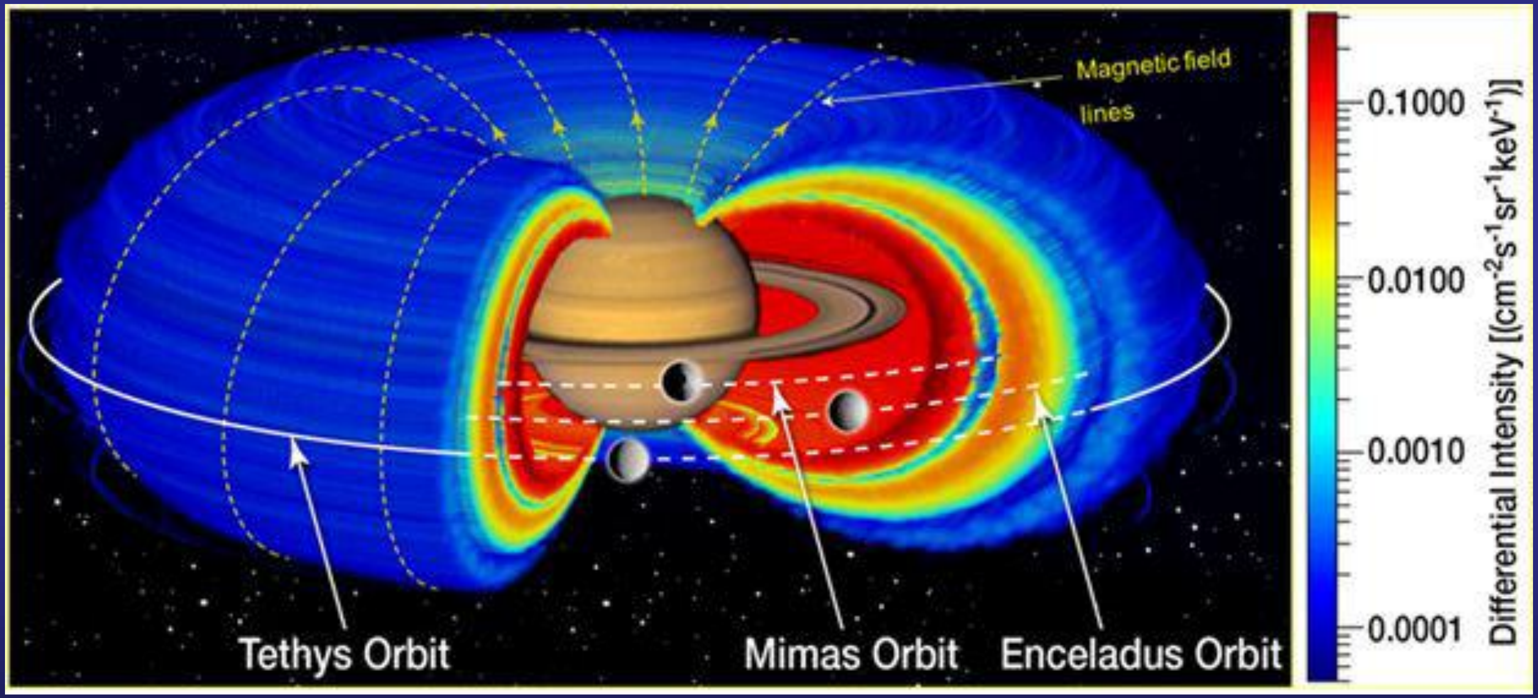

E.2 Plasma processes in Jupiter‘s magnetodisk

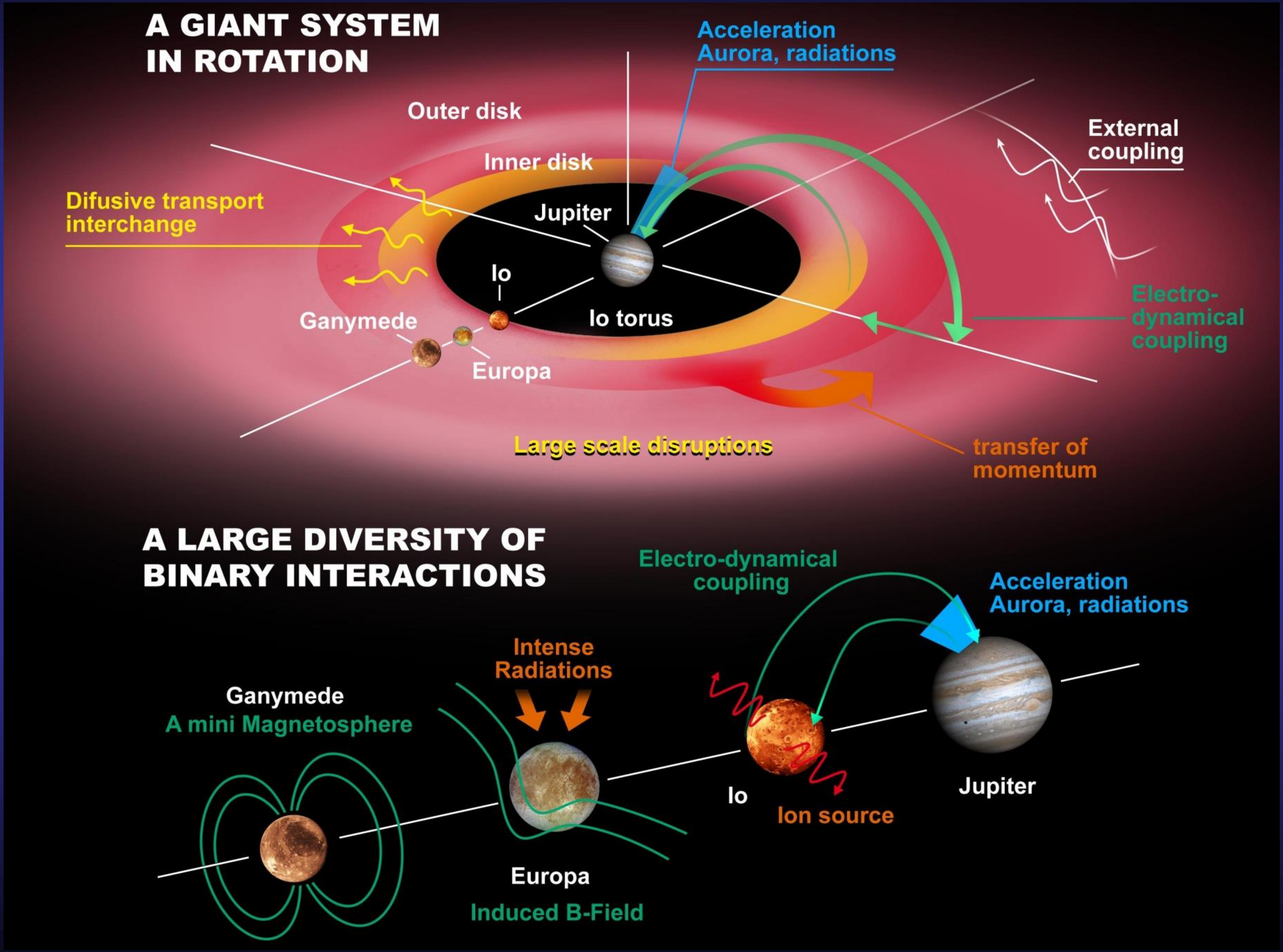

E.2 Global plasma flow patterns in Jupiter's equatorial plane (Galileo-EPD results)

(sub)-corotational flows out to 150 RJ

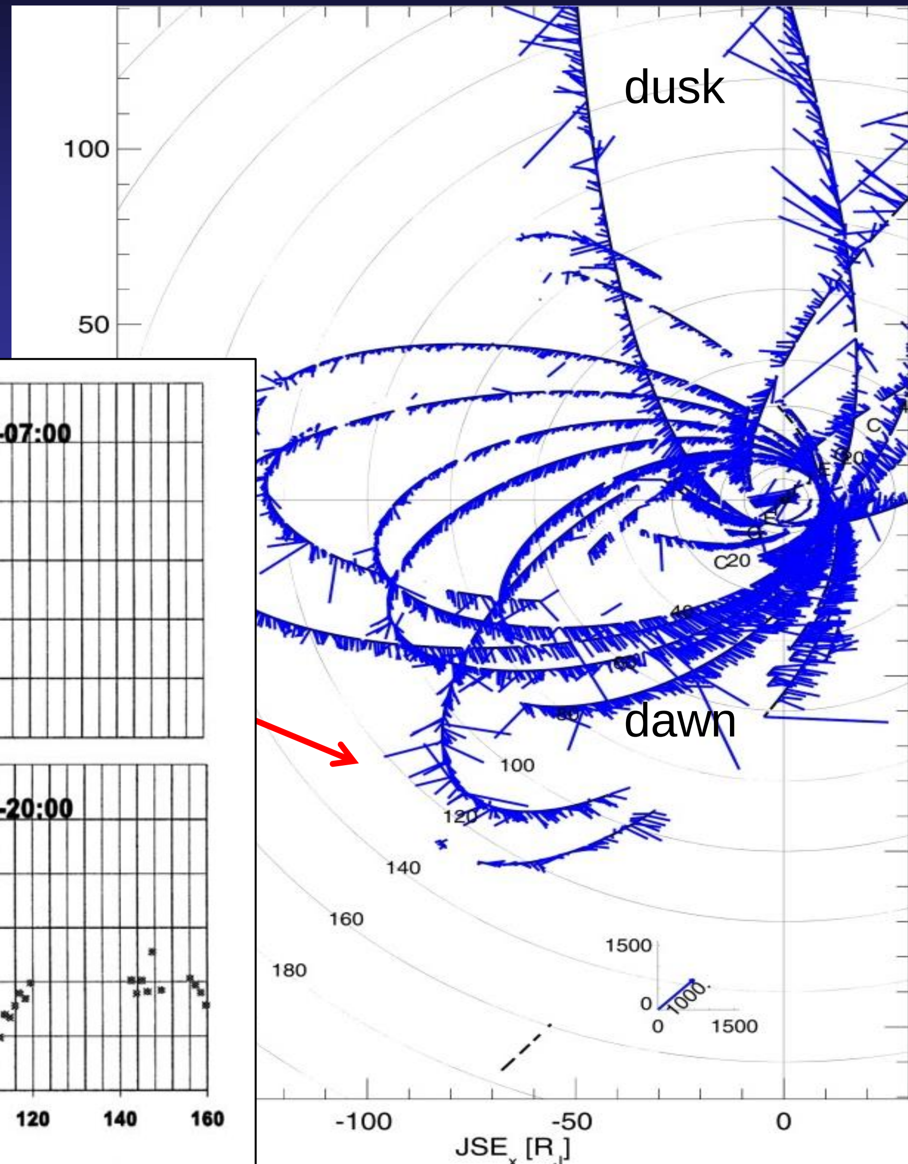

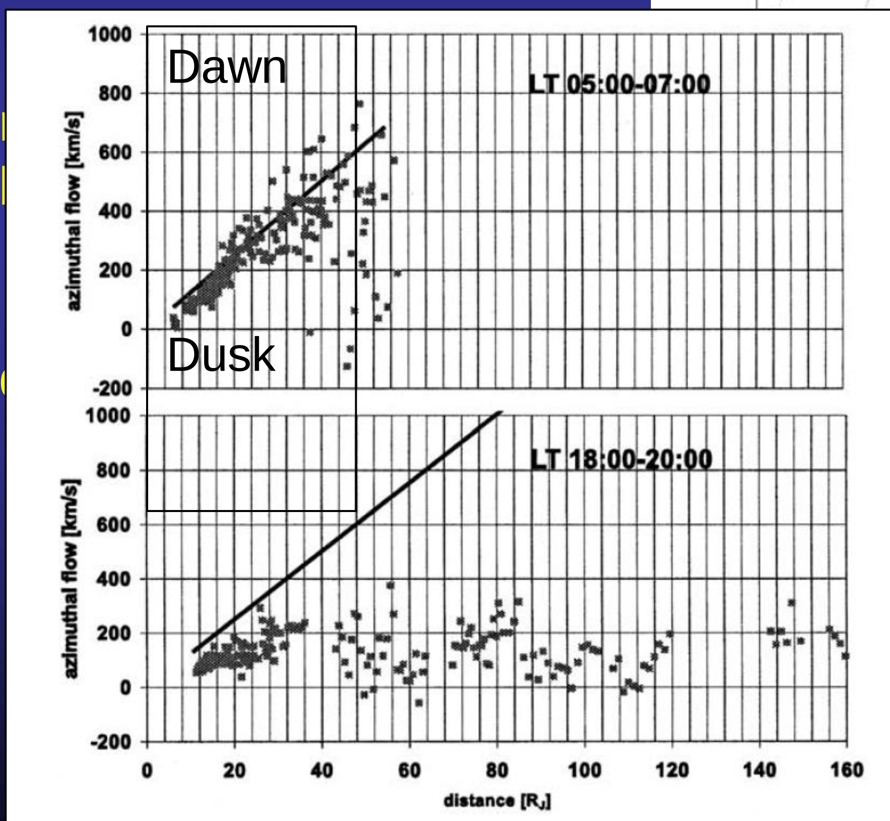

Sun →

E.2 Interchange / Injections events at Jupiter
Signatures in energetic particles

Possible observation of interchange flux tubes

Local enhancement of density.
seen by wave and magnetic signatures

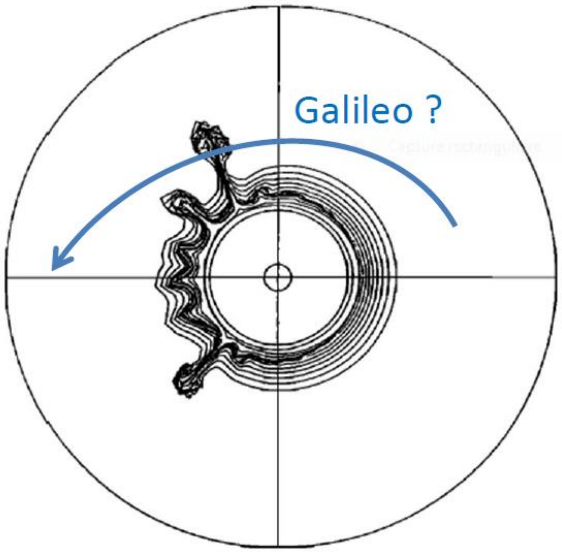

Simulation of torus-driven plasma transport in the jovian magnetosphere, Yang et al, JGR, 1994

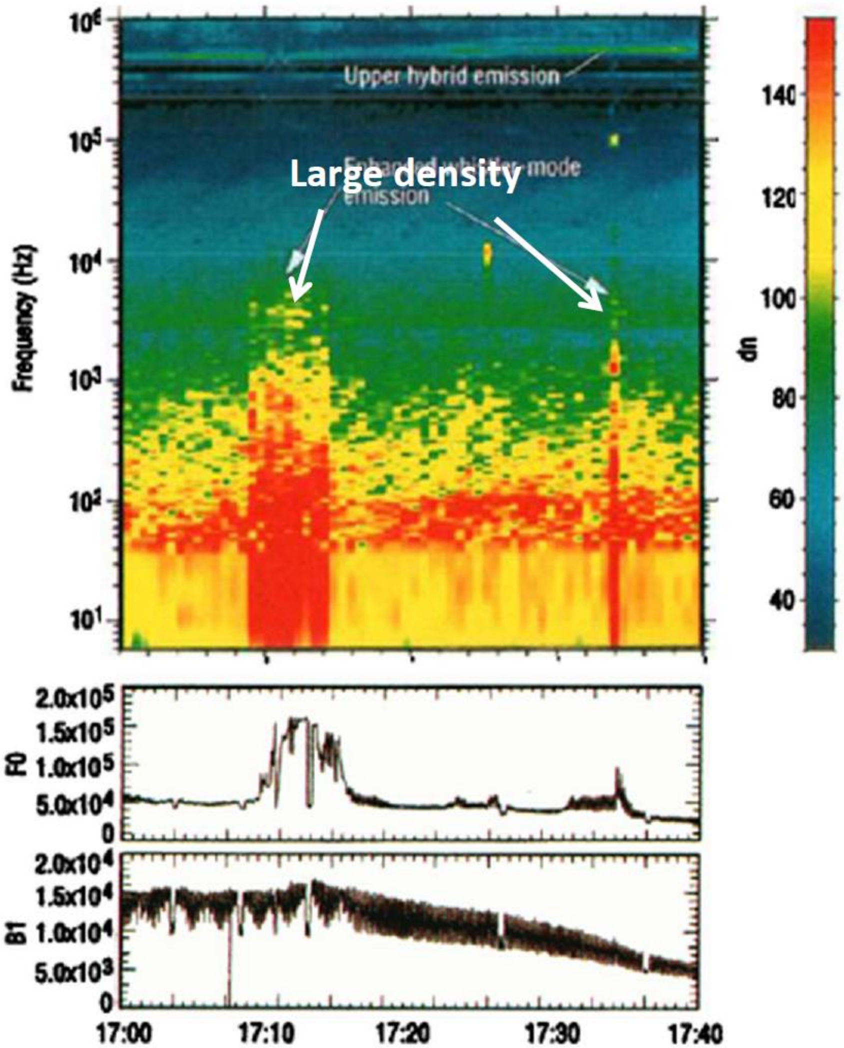

Bolton et al , 1997

MAX-PLANCK-GESELLSCHAFT

E.2 Particle Injections in Jupiter's magnetosphere energetic particle signatures (Mauk et al., 1997, 1999)

MPS
Max-Planck-Institut für Sonnensystemforschung

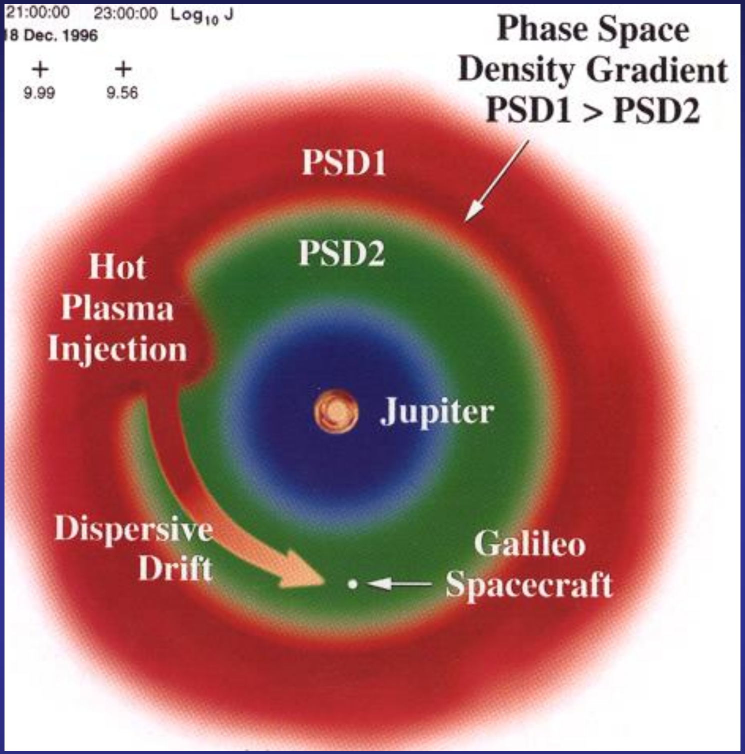

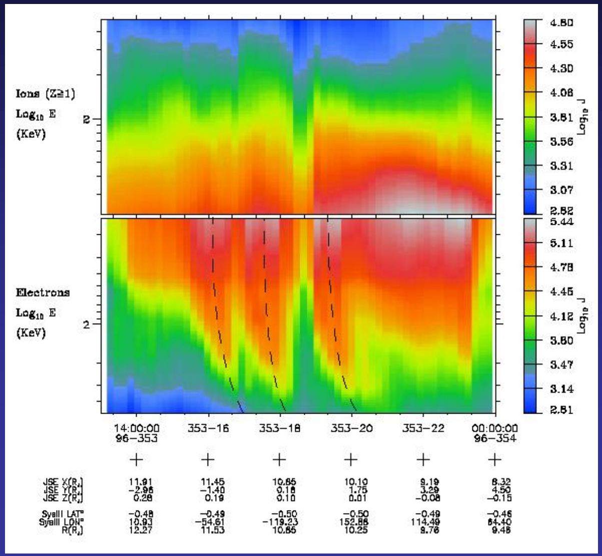

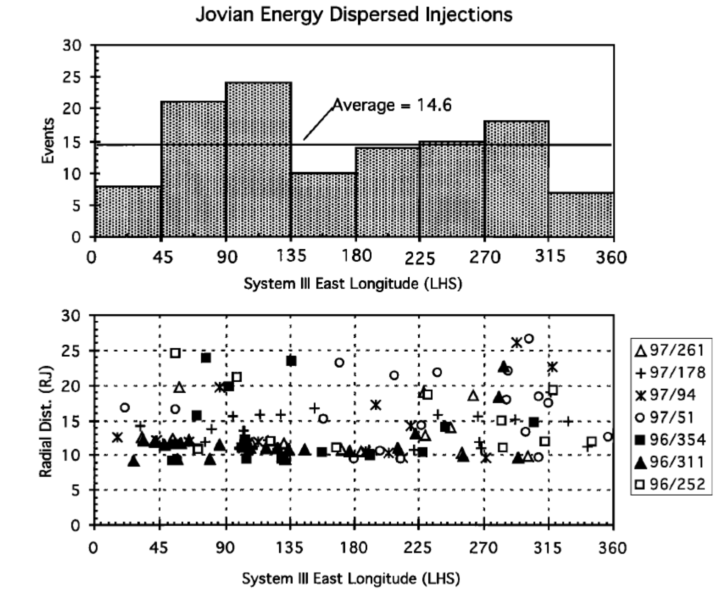

The behaviors of Jupiter magnetosphere injections were understood by invoking sudden radial injections over confined regions in azimuth followed by slow, dispersive, azimuthal drifts.

E.2 Plasma transport processes in Jupiter's magnetosphere, hot plasma injections

- > 100 analyzed (more in the Galileo data)
- observed between 9-27 RJ with a peak @ 11-12 RJ
- observed @ all LT (with a tendency of more in the nightside ?? → biased by S/C trajectory)
- can be clustered in time (storm-like) with correlated signatures in auroral emissions

Galileo/EPD energy vs. time spectrogram

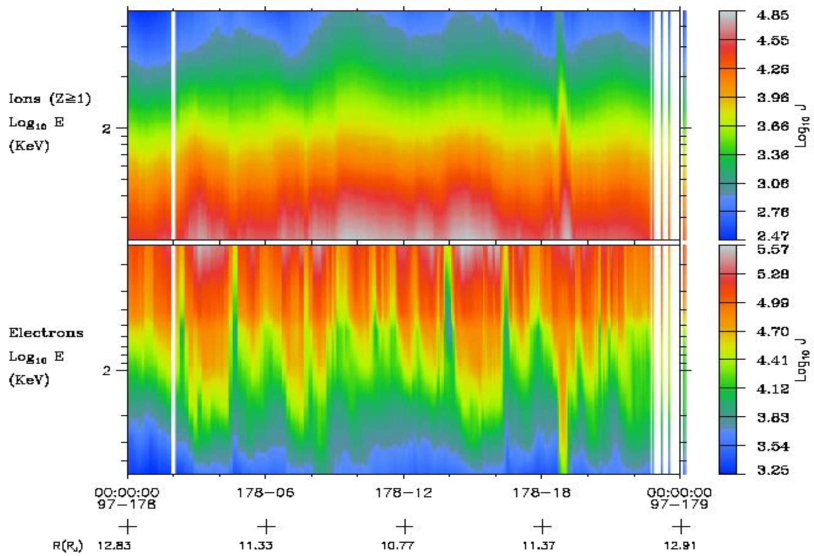

Extreme "storm-time" dynamics observed in the vicinity of Europa's orbit

HST UV aurora

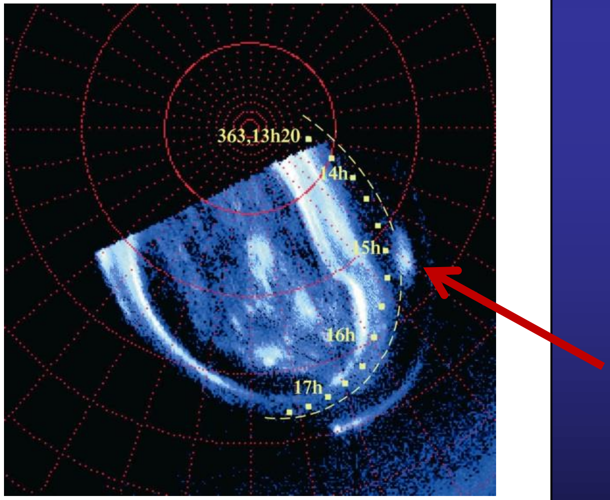

Mauk et al., 1997; 1999, 2000

Auroral manifestation of near-Europa storm dynamics

E.2 “Substorms” in Jupiter’s magnetosphere

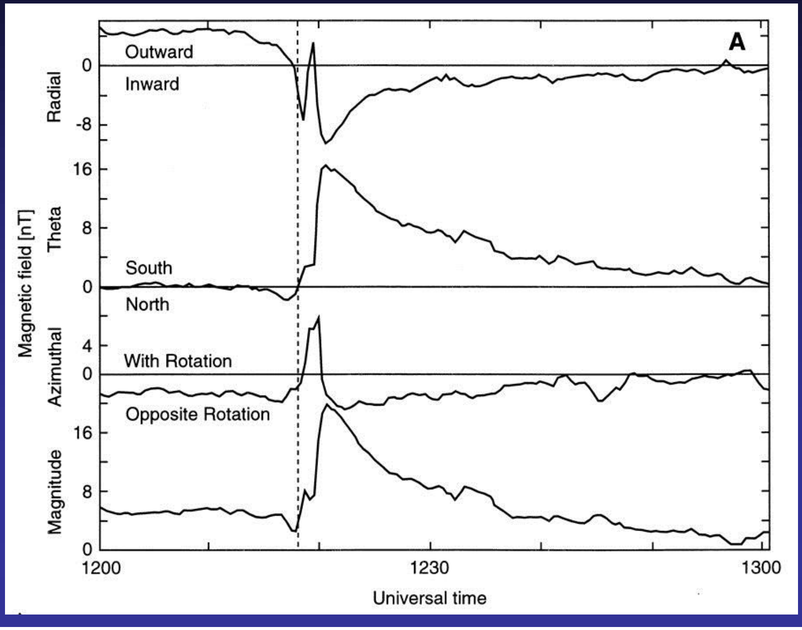

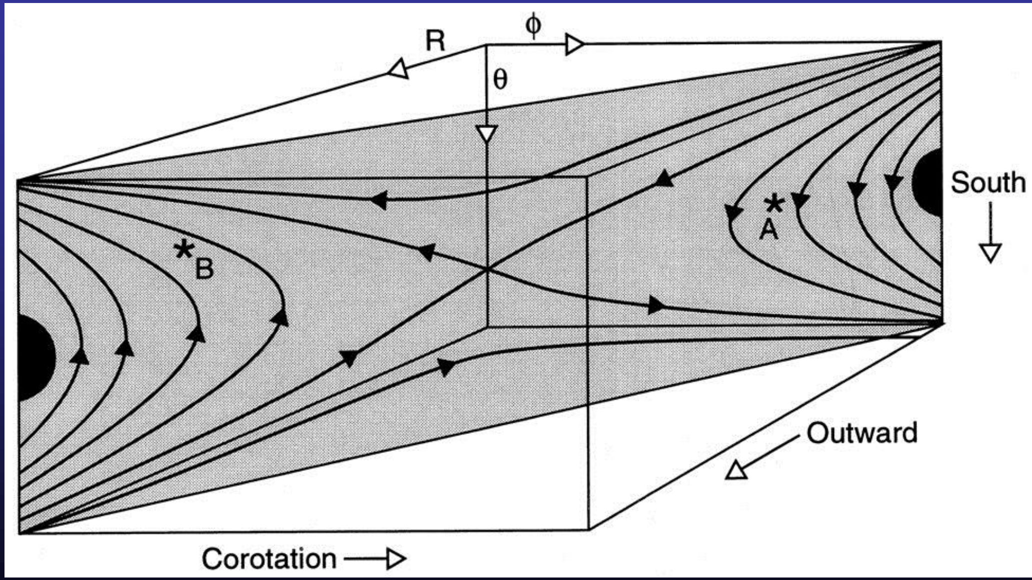

–first evidence in Voyager data (Nishida, 1983)

–Russell [Adv. Space Res., 2000, 2002] provides evidence for reconnection in the magnetotail.

–The enhanced southward field accompanied by Jupiter planetward flows and enhanced northward field accompanied by tailward flow.

–Most of the reconnection events were seen in the dawn sector.

–In accord with the study of Krupp et al. [2001] who saw flow bursts mostly in the dawn sector.

E.2 Particle bursts in Jupiter's magnetotail
Krupp et al., 1998; Woch et al., 1998, Louarn et al., 2001

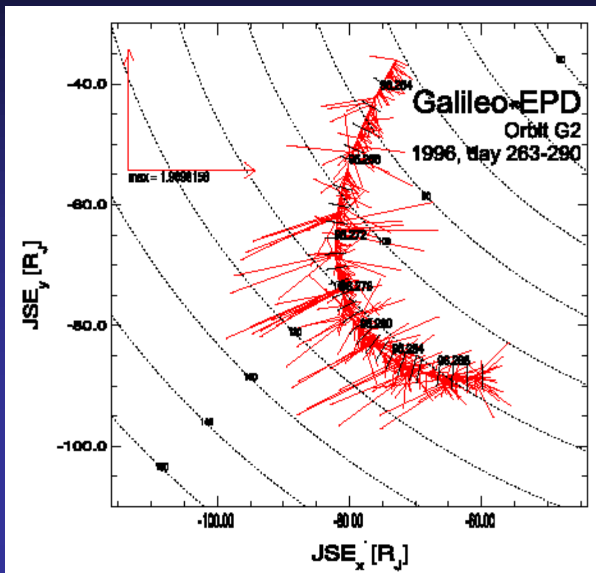

periodicity
of 2-3 days

in particles, MAG,
plasma waves

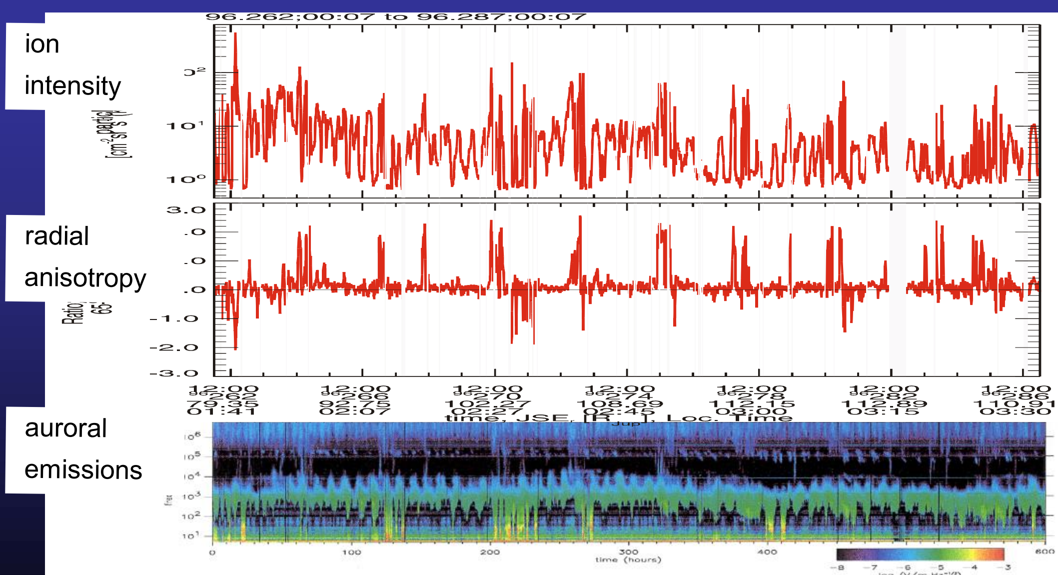

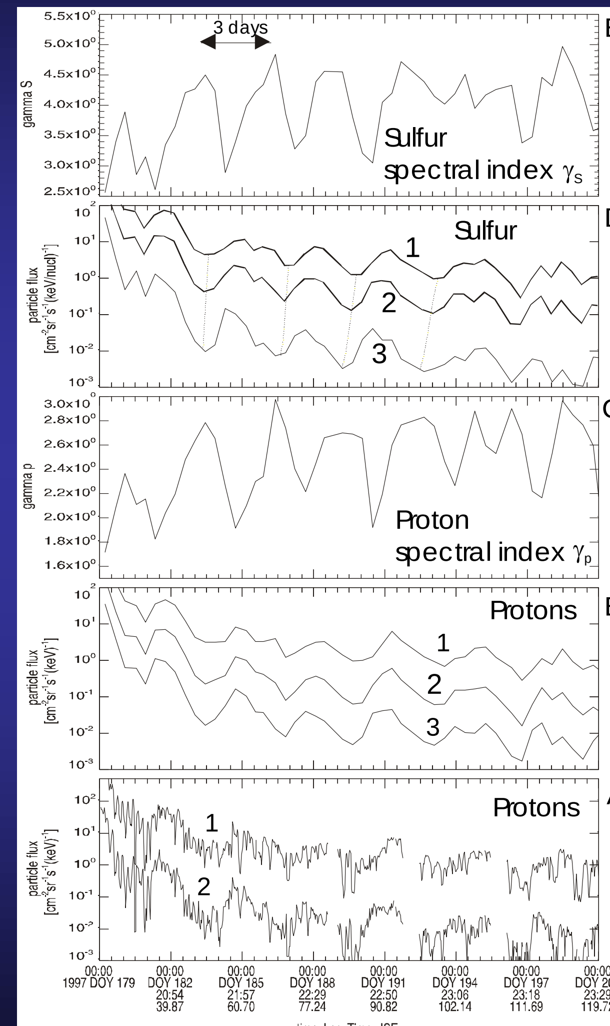

E.2 Reconnection events in the Jovian magnetotail

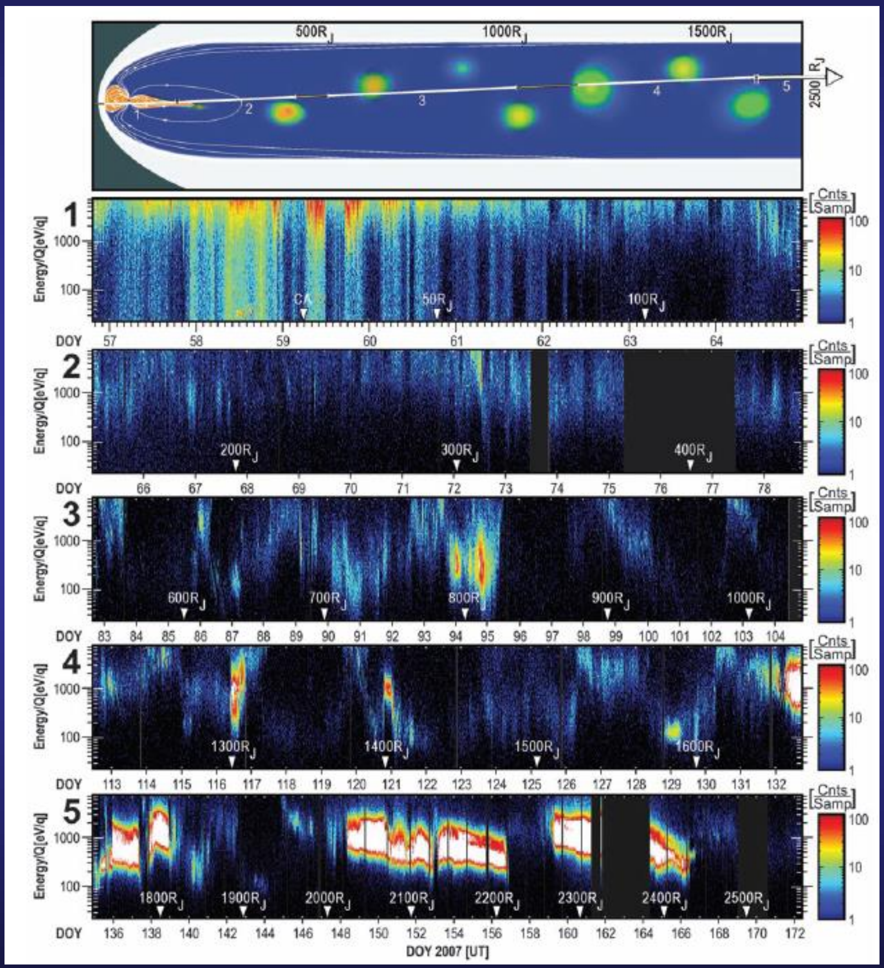

McComas, 2007

249 events in Galileo/Mag (Vogt 2010) correlated with 34 in Galileo/EPD particle data (Kronberg 2005, 2007)

observed > 30 RJ

statistical x-line 60-90 RJ at dawn and 90-120 RJ pre-midnight

2-3 days periodicity

plasmoid signatures observed beyond 1500 RJ with New Horizons S/C

E.3 Jupiter‘s aurora – a „camera“ for magnetospheric activity

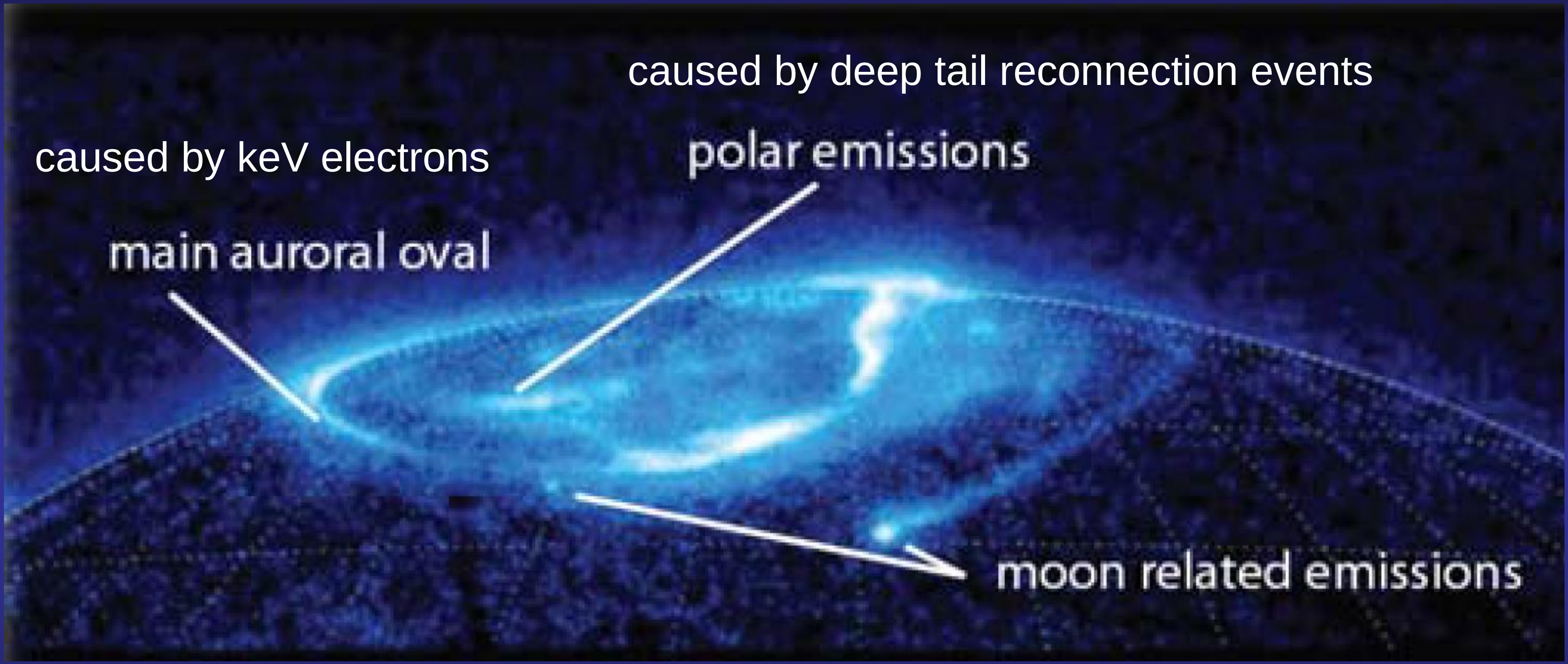

Corotation breakdown → main auroral oval
Processes in the magnetotail → polar emissions
plasma processes near the moons → moon related emissions

E.4 Plasma processes near the moons

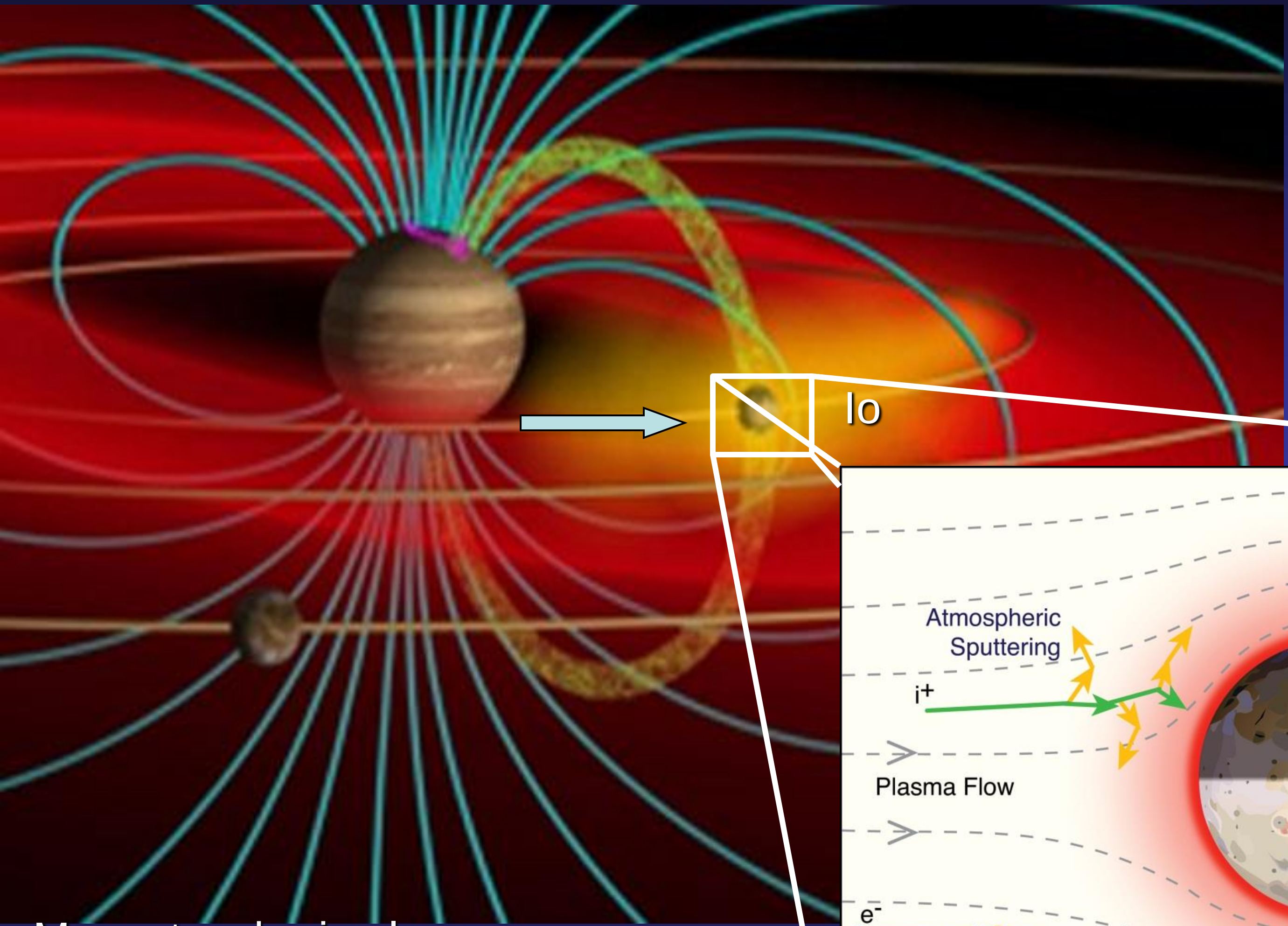

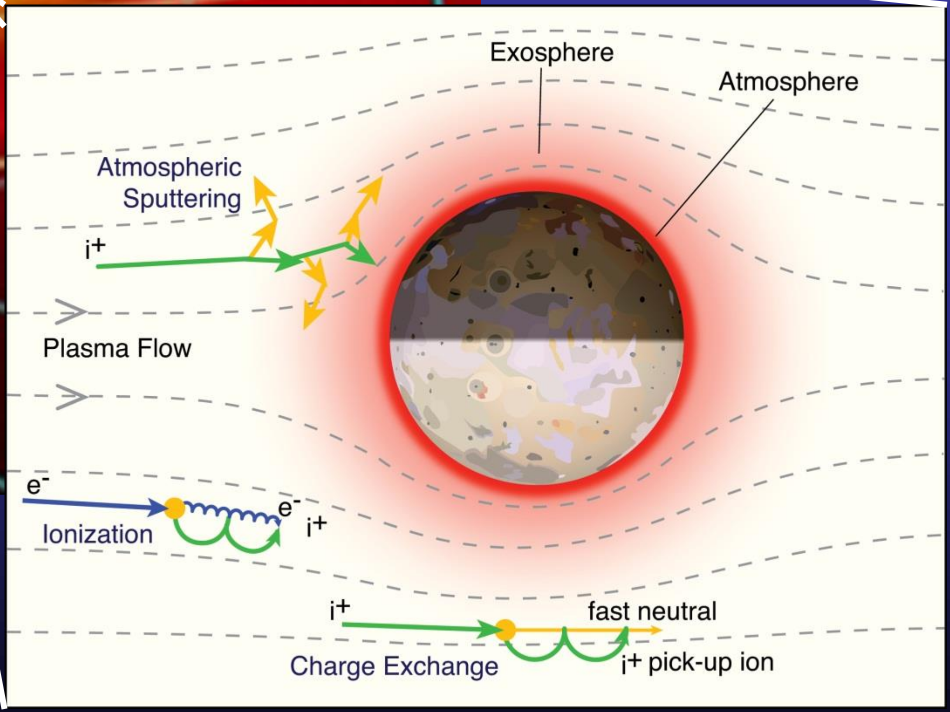

Plasma = hot, ionized gas

Magnetospheric plasma interacts with Io's atmosphere

E.4 Ganymede's mini-magnetosphere within the huge Jovian magnetosphere

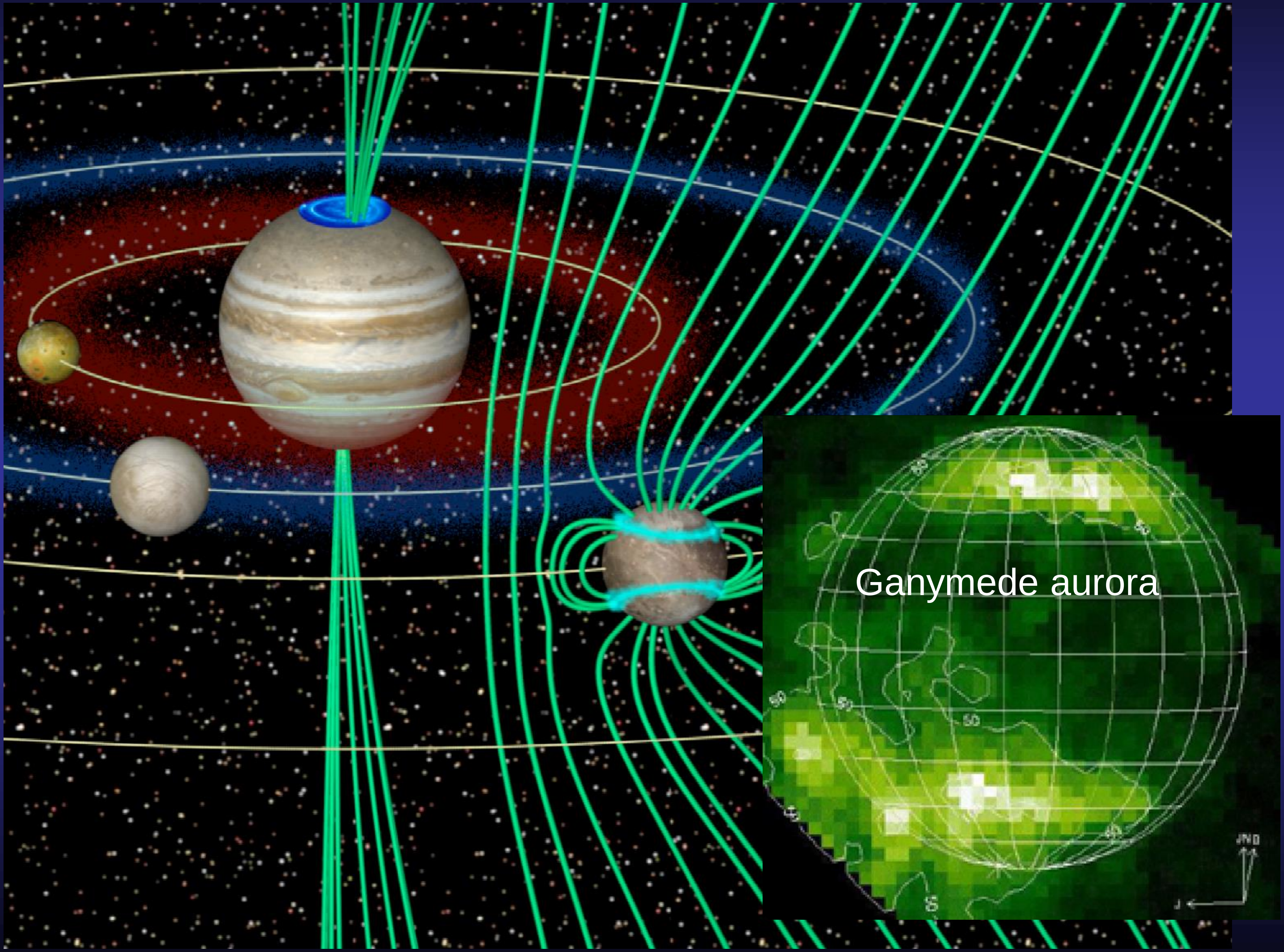

E.4 Energetic particles in planetary magnetospheres
4. Useful tool to study plasma processes

a) discovery or identification of unknowns objects (moons, plumes, rings, ring arcs, neutral clouds)
b) determination of diffusion coefficients
c) determination of flow velocities
d) characterization of electric fields
e) determination of open-closed fieldline boundaries in the auroral region
f) surface weathering of moons
g) remote sensing of surfaces
h) global „imaging“ of magnetospheric dynamics with ENA

E4a: discovery of unknown objects
Discovery of Europa neutral gas torus

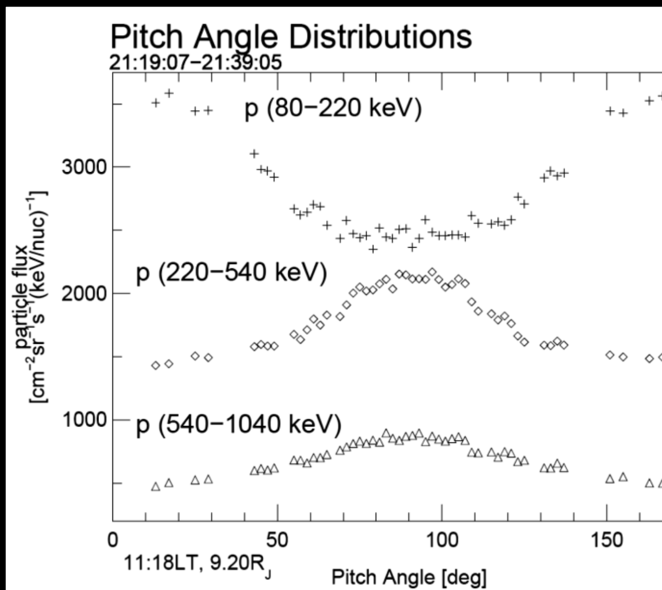

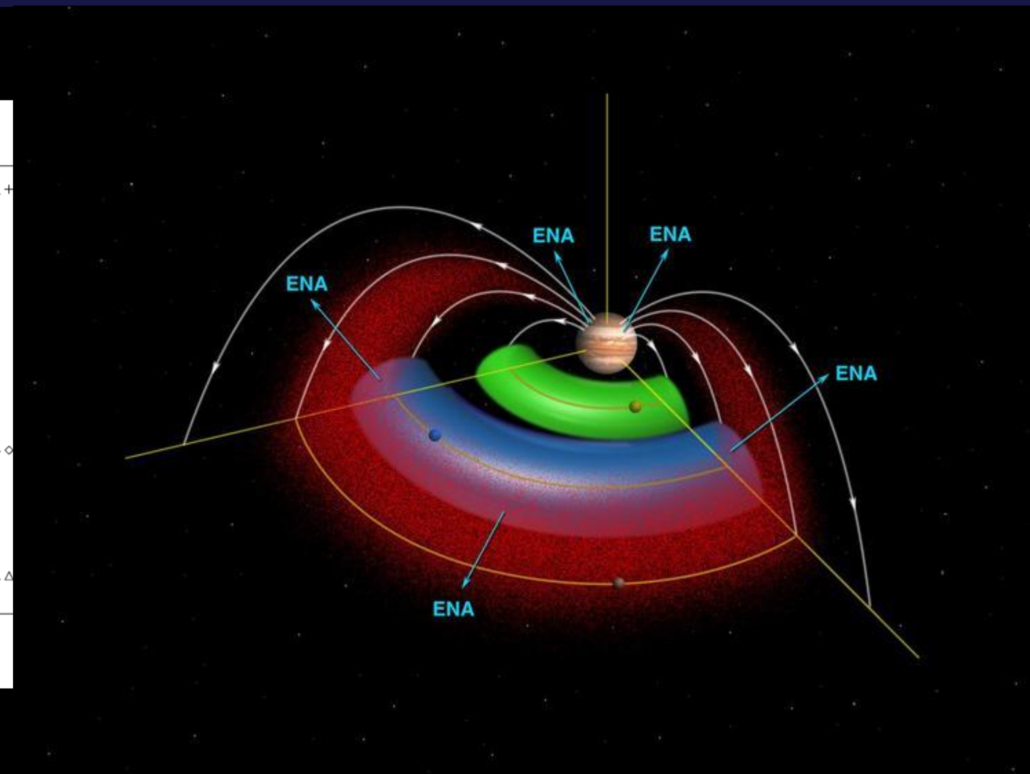

neutral density in the Europa-Torus from changes in the pitch angle distributions of energetic particles: Galileo/EPD results (Lagg et al., 2003)

Direct ENA measurements from Cassini only from far away (Mauk et al. 2003)

E4a: discovery of unknown objects
Simulated Europa neutral torus

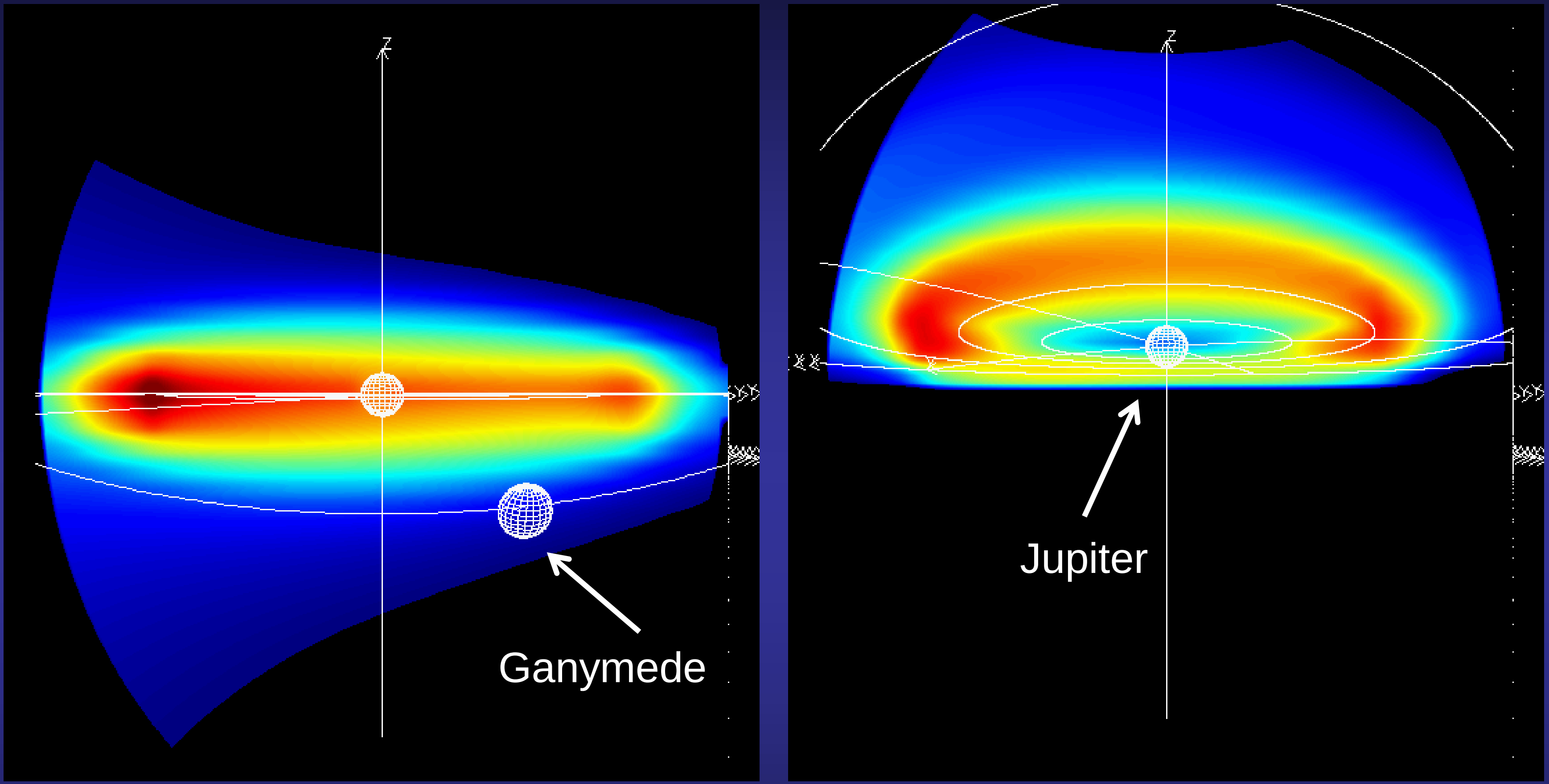

Expected ENA emissions from the EUROPA torus as viewed from a JUICE orbit (P. Brandt)

E4b: Determination of diffusion coefficients extraction via moon electron microsignatures

van Allen, 1980; Roussos, 2007

Diffusion equation

x: displacement of absorption from the center

$$f = 1 - 0.5\left[erf\left(\frac{1 - x/R}{\sqrt{\tau}}\right) + erf\left(\frac{1 + x/R}{\sqrt{\tau}}\right)\right]$$

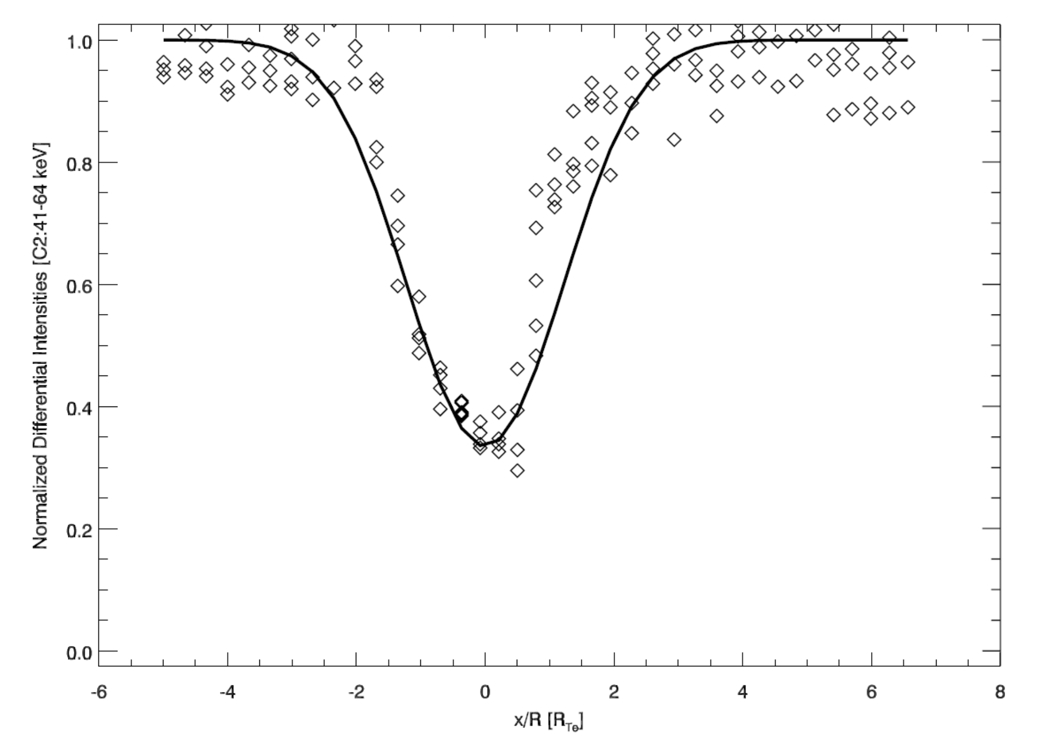

$$\tau = 4D_{LL}t_{rk}/R^2 .\ D_{LL}$$

$$D_{LL} = D_o L^n$$

diffusion coefficient

n =10 magnetic fluctuations

n=6 electric field potentials

E4b: Determination of diffusion coefficients
radial diffusion coefficient in Saturn's magnetosphere

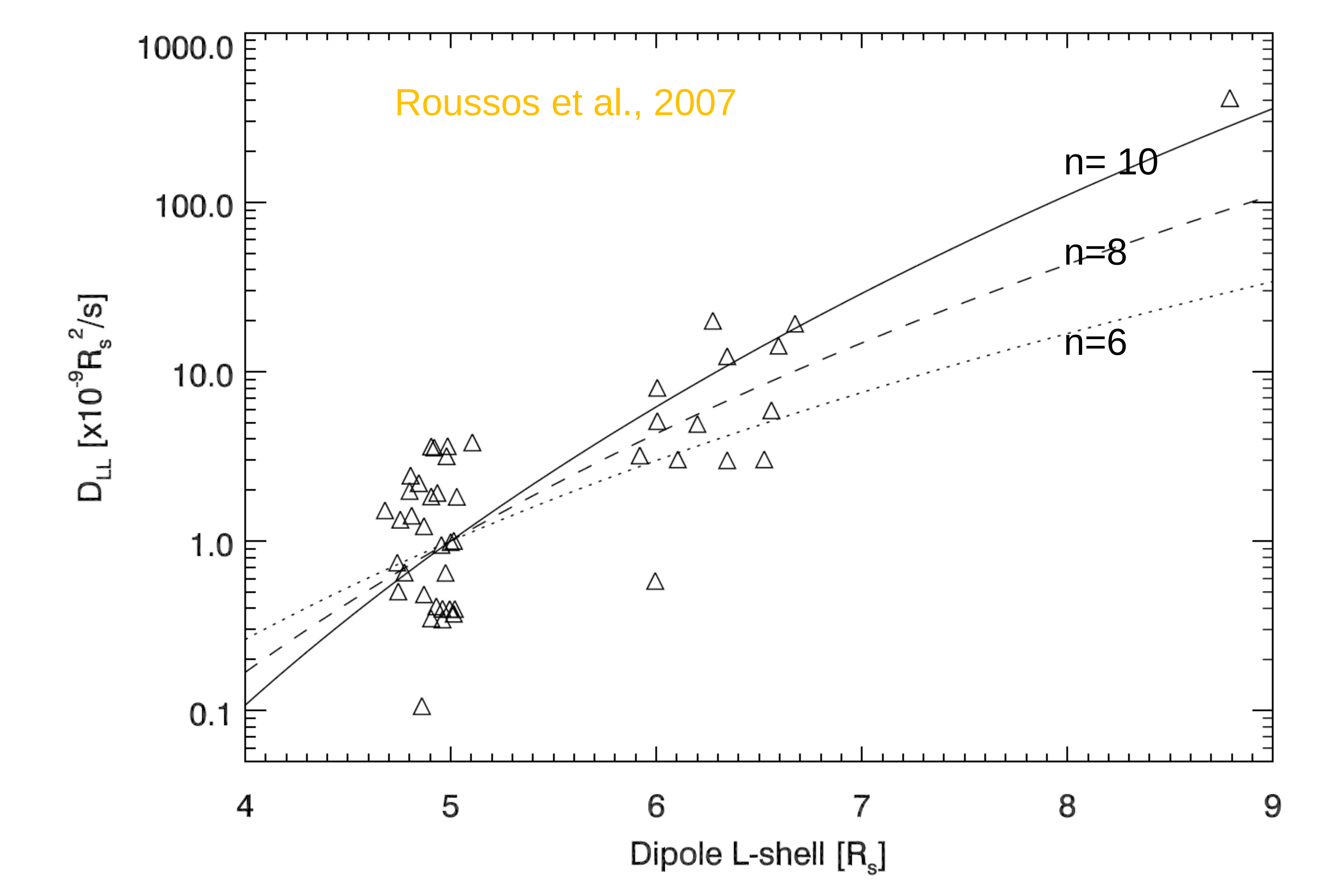

E4c: Determination of flow velocities

$$I_{\text{omni}}(E) = I_0 \left(\frac{E}{E_0}\right)^{-\gamma}$$

$$I(E,\vartheta,\varphi) = I_{omni} \sum_{n=0}^{\infty} \sum_{m=-n}^{m=n} A_{nm}(E) Y_{nm}(\vartheta,\varphi)$$

$$\ln[I(E,\varphi)] \propto \frac{2v_F}{v_{\text{ion}}} \cos\varphi$$

$$Y_{nm}(\vartheta,\varphi) = P_{nm}(\cos\vartheta)\cos(m\varphi) \quad m > 0$$
$$Y_{nm}(\vartheta,\varphi) = P_{n|m|}(\cos\vartheta)\sin(|m|\varphi) \quad m < 0$$

$$\mathbf{A_1} = \mathbf{A_F} + \mathbf{A_G} + \ldots.$$

$$\mathbf{A_G} = \frac{m \cdot v_{\text{ion}}}{q \cdot B^2} \cdot \left(\mathbf{B} \times \frac{\nabla I}{I_{omni}}\right)$$

$$\mathbf{A_F} = \frac{2(\gamma+1)\mathbf{v_F}}{v_{\text{ion}}}$$

$$\mathbf{v_F} = \frac{\mathbf{A_F} \cdot v_{\text{ion}}}{2 \cdot (\gamma+1)}$$

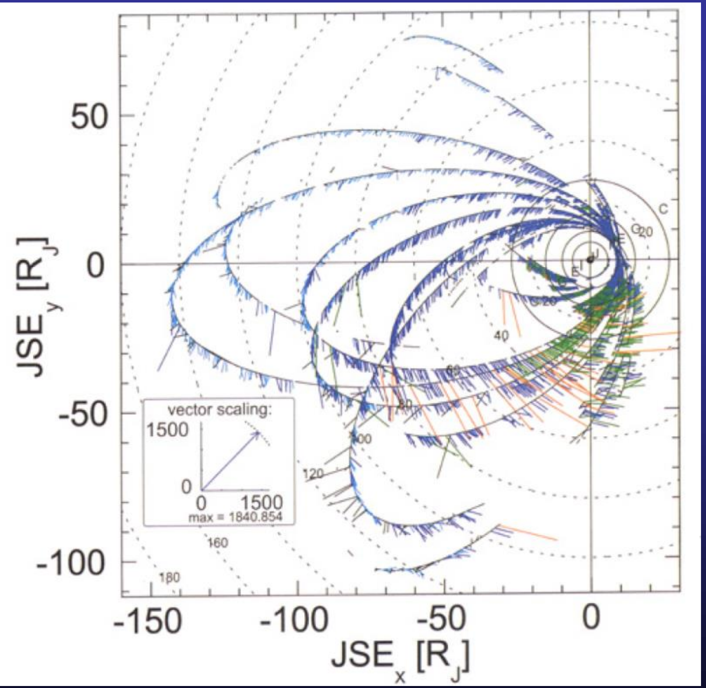

Krupp et al., 2001

E4d: Characterization of electric fields

expected moon microsignature

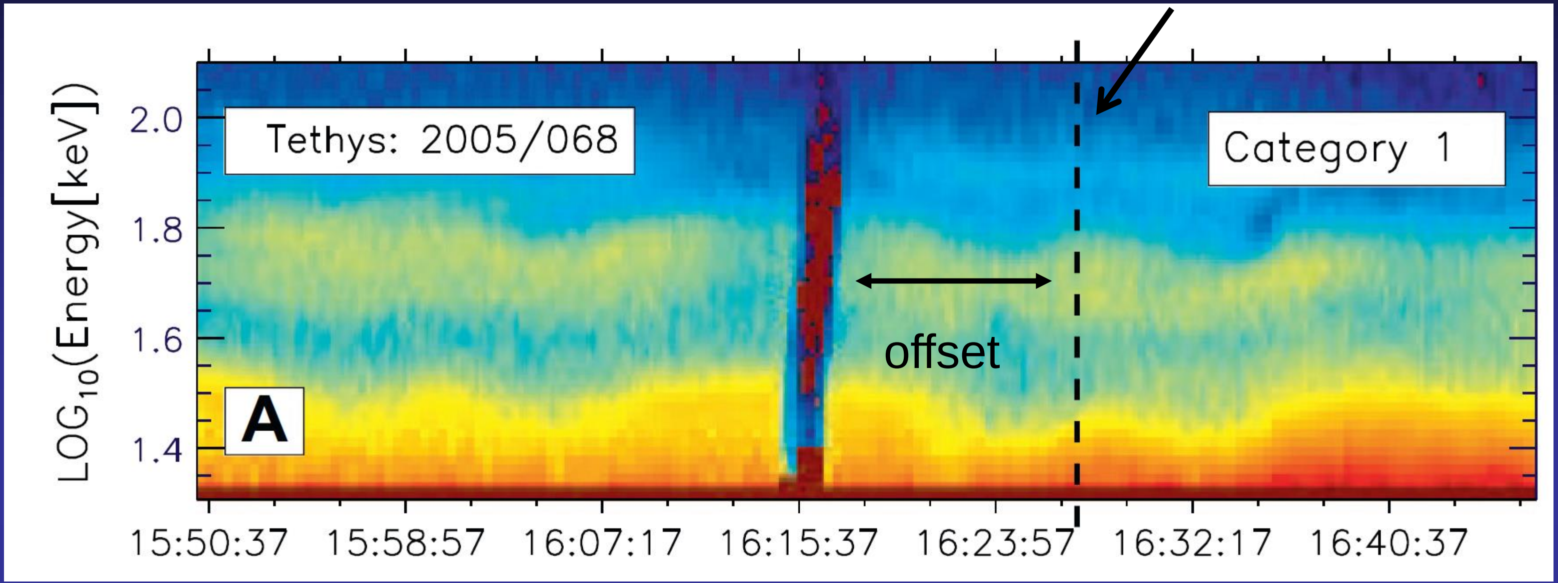

electron spectrogram

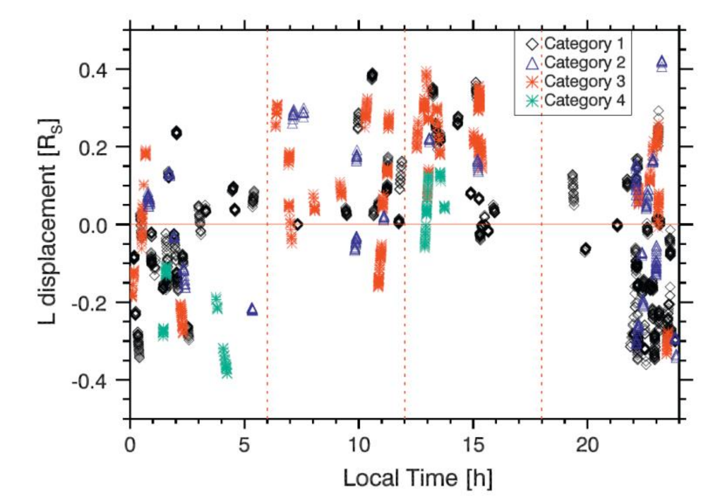

Nightside: inward displacements
Dayside: outward displacements

→ Electric field in the noon-midnight orientation

E4e: Determination of open closed fieldline boundary

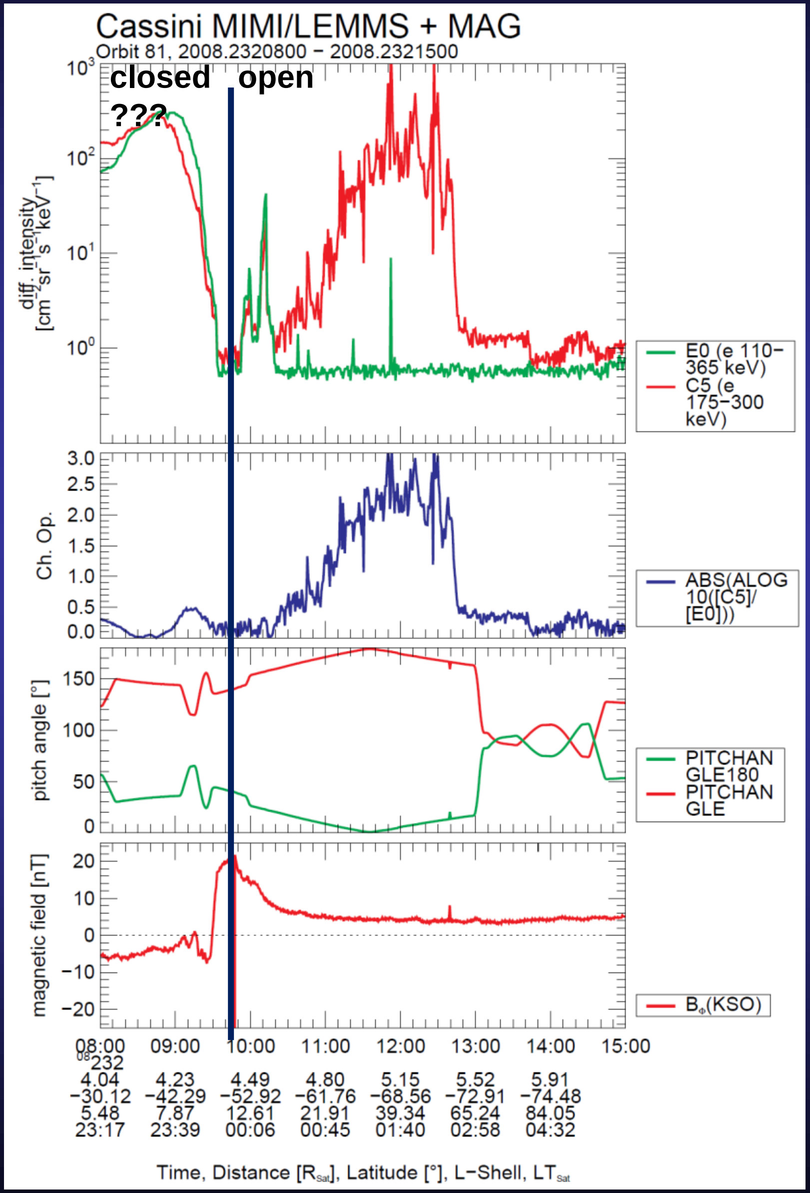

Field-aligned particle distributions are used to map the open-closed fieldline boundary

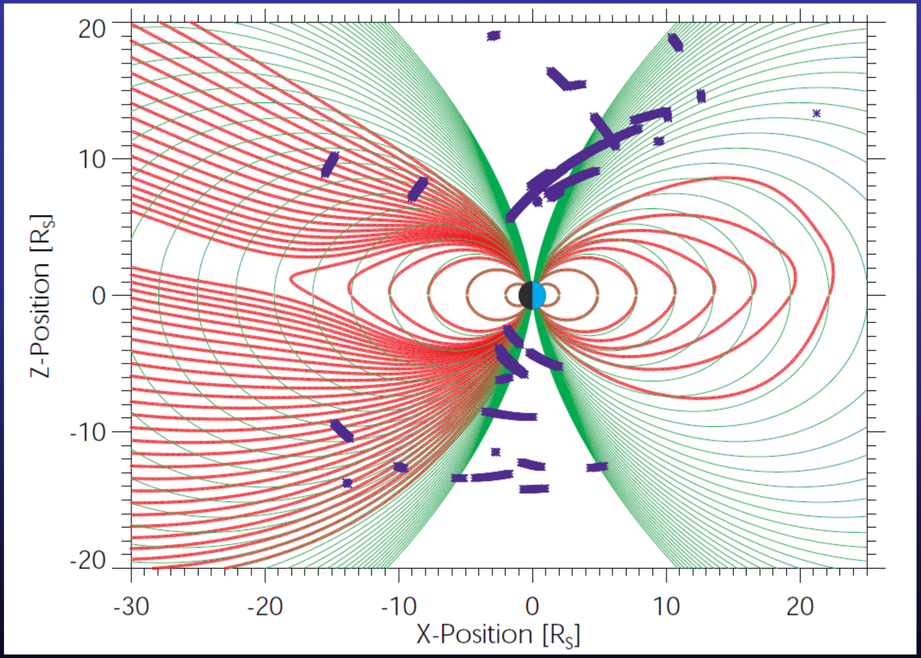

E.4 Plasma interaction between Jovian magnetosphere and moons

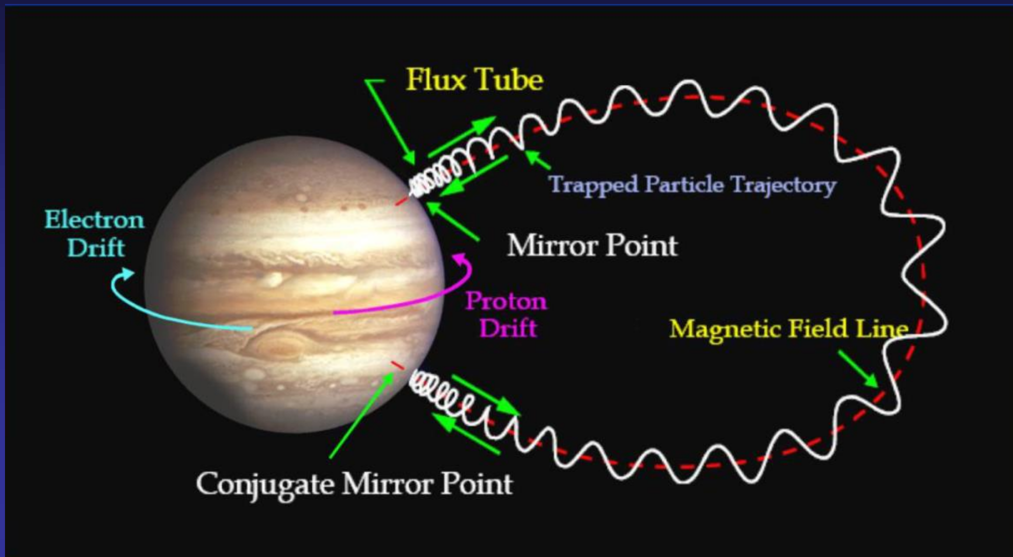

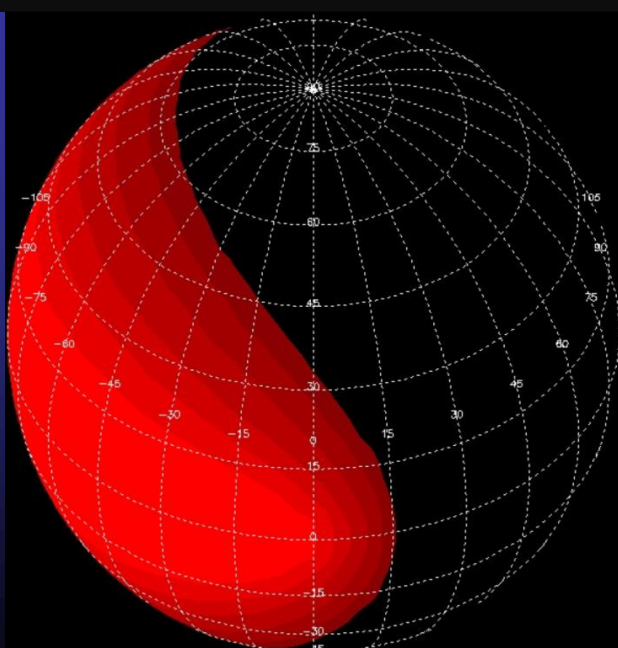

If the magnetosphere of Jupiter is rigidly co-rotating, plasma flow speed at Europa’s orbit (9.5 Rj) is about 118 km/s.
Europa travels about 14 km/s in its orbit, so that charged particles are overtaking the satellite at all times.

E4. f Surface weathering

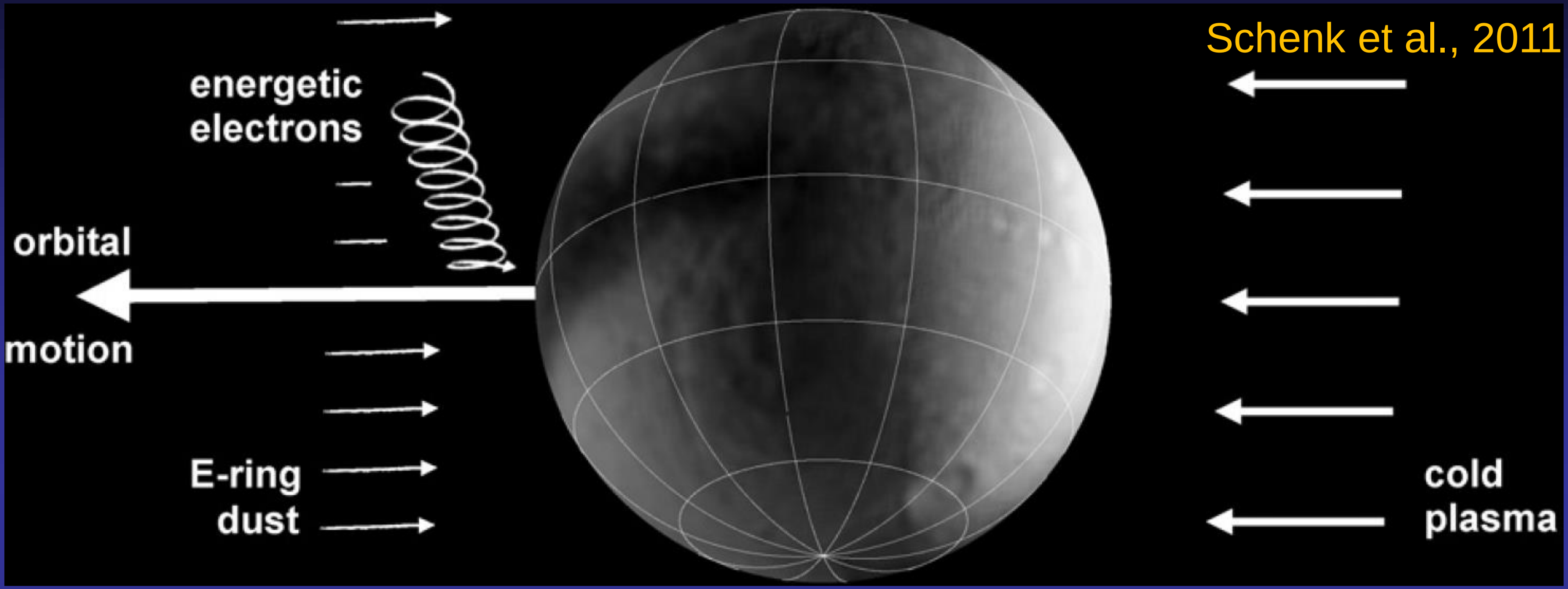

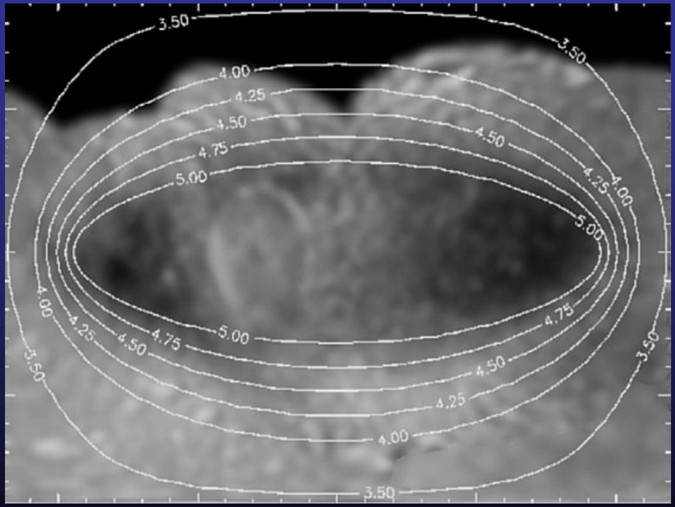

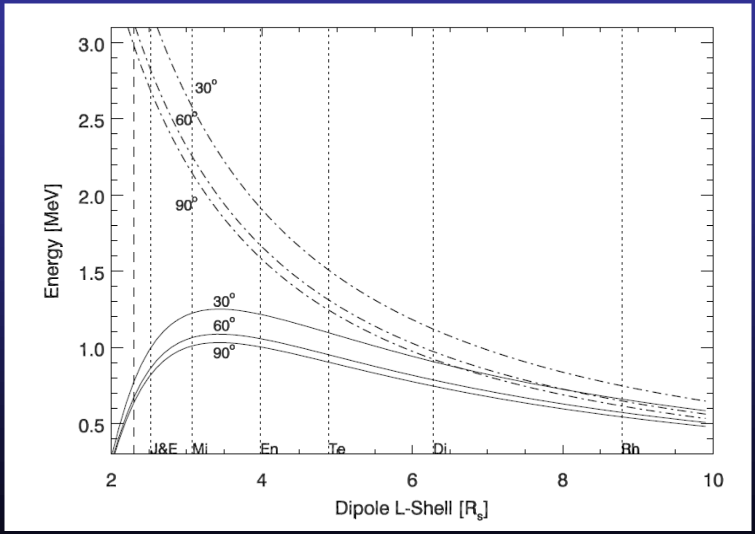

E. Jupiter
key regions and magnetospheric interactions

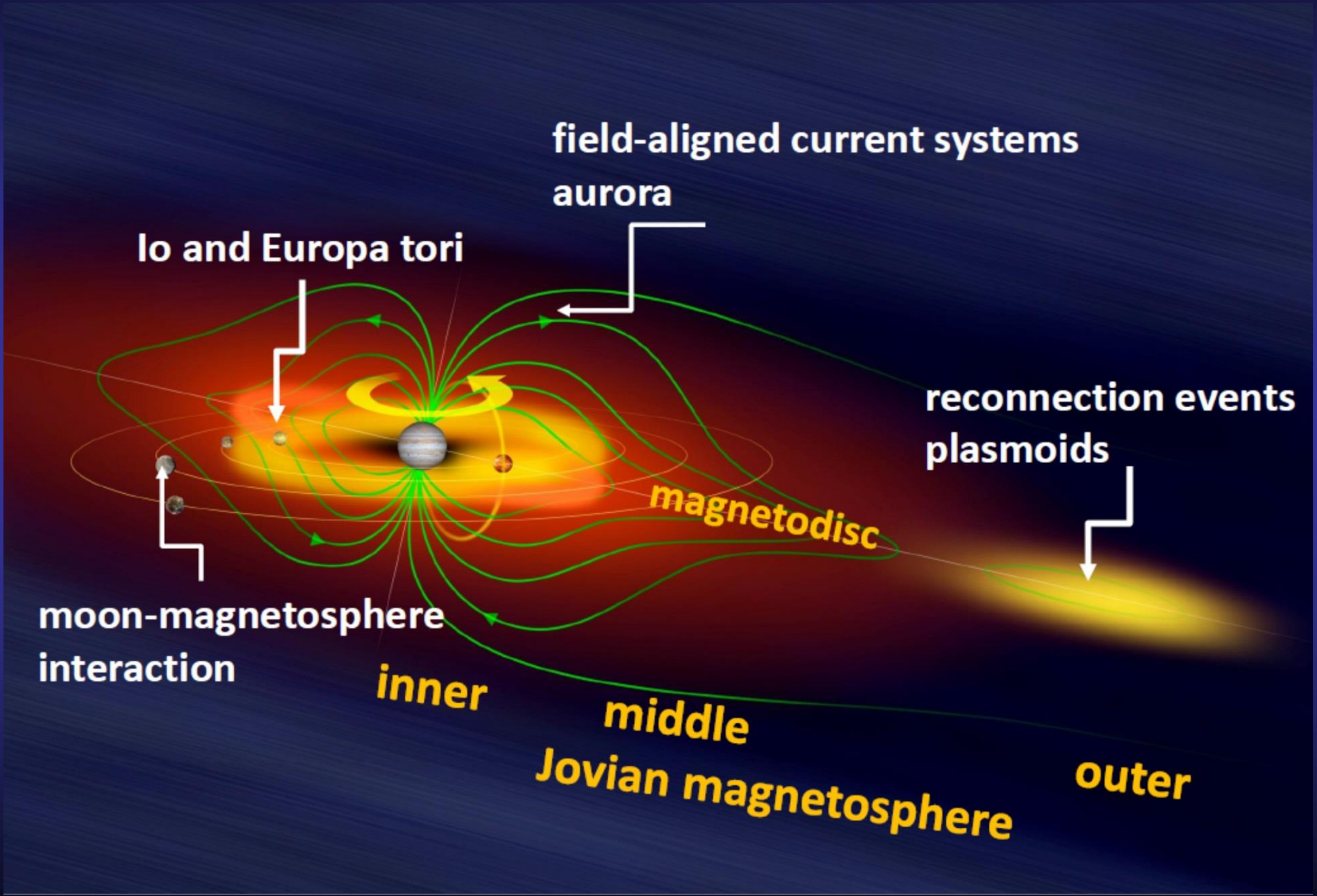

E. Saturn
key regions and magnetospheric interactions

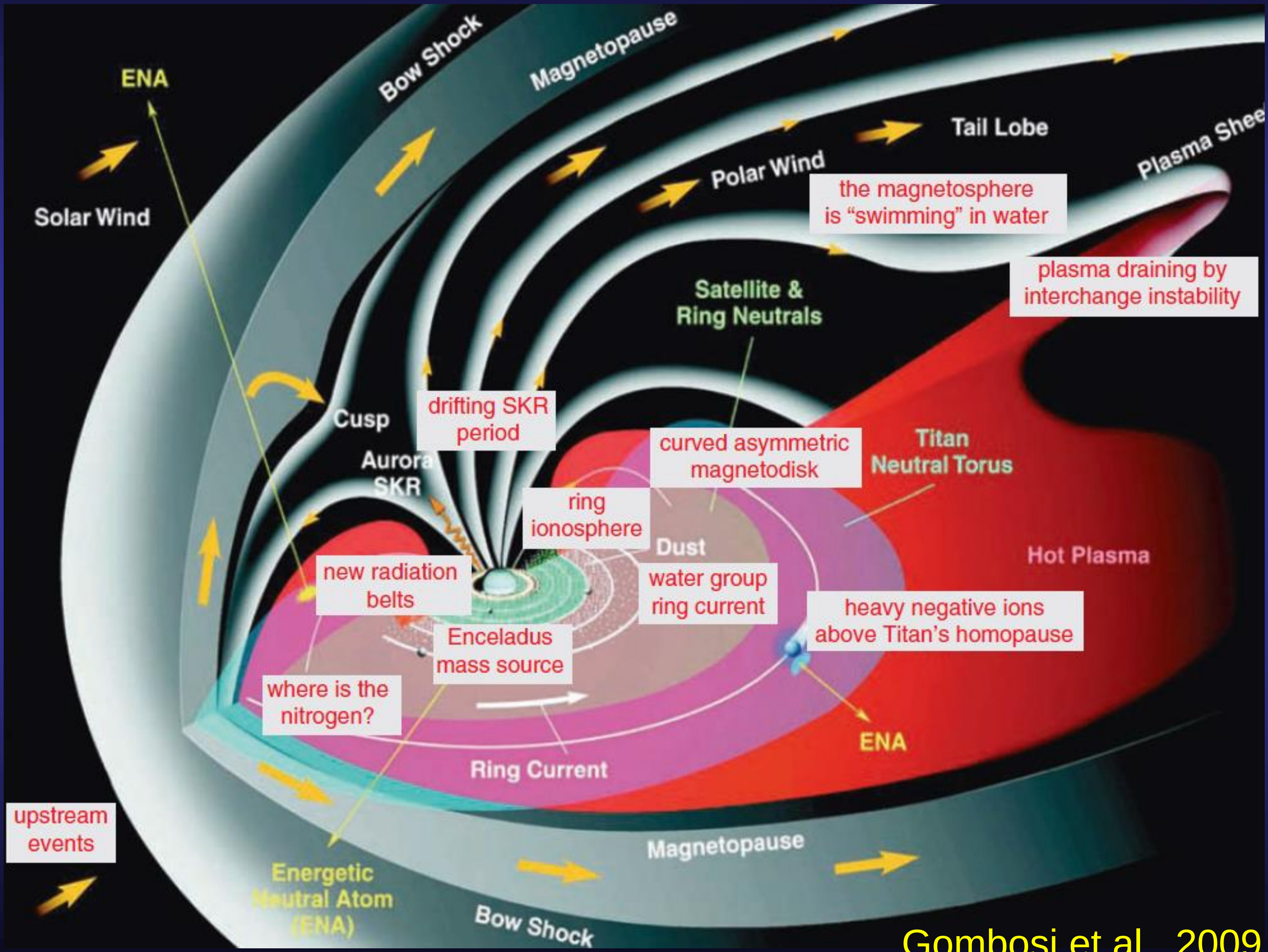

Gombosi et al., 2009

E. Jupiter
density, pressure, plasma beta (Mauk et al, 2004)

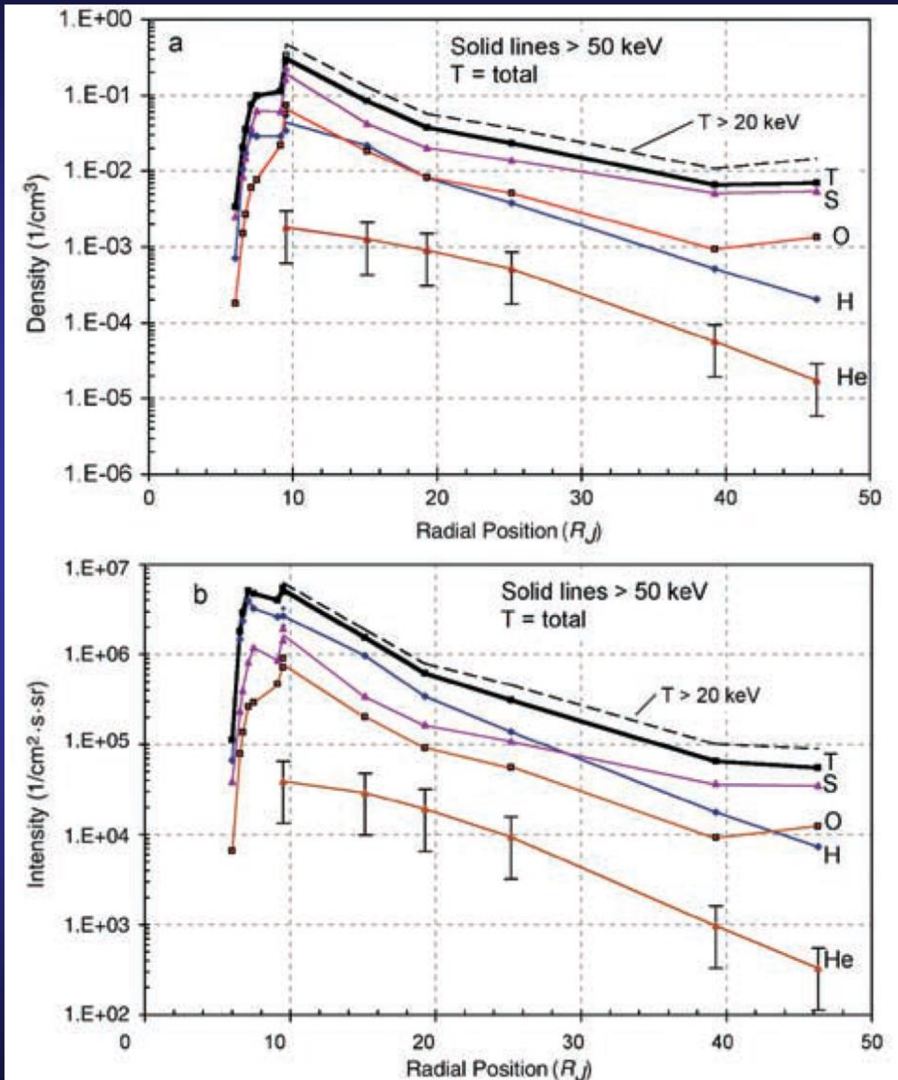

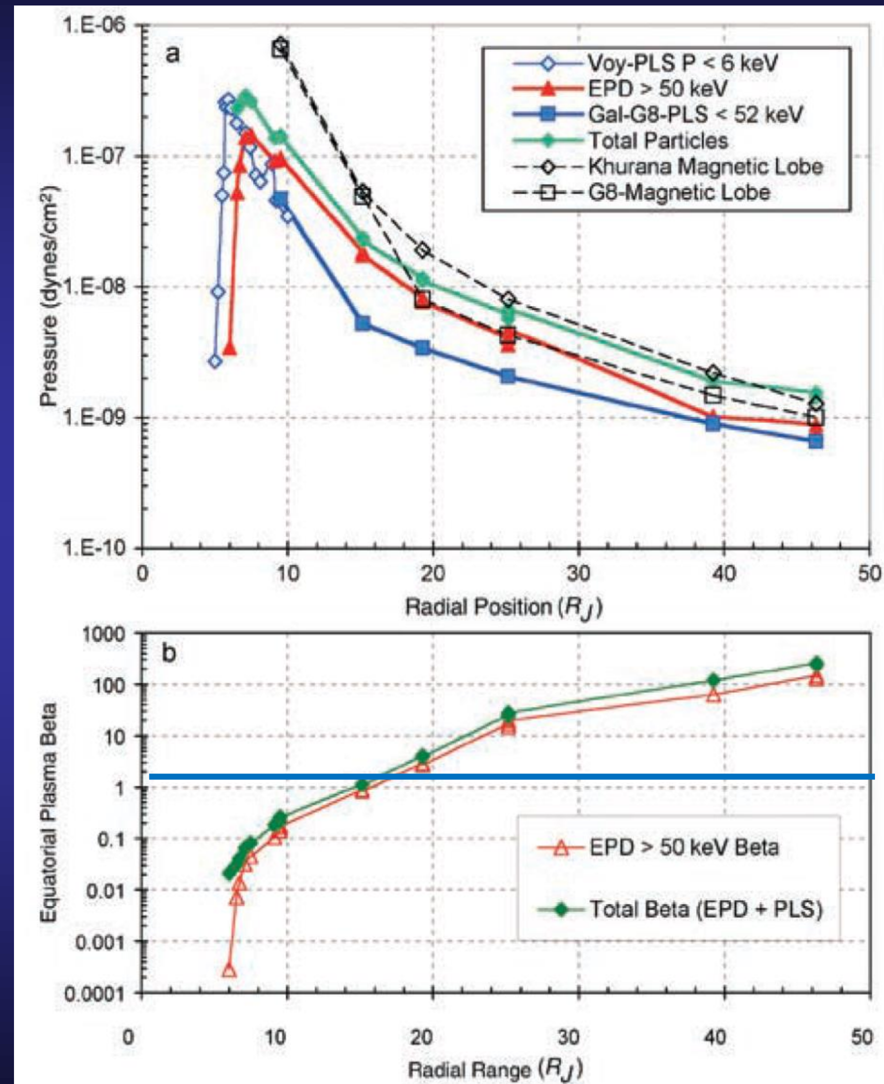

E. Saturn
pressure, plasma beta (Sergis et al, 2007)

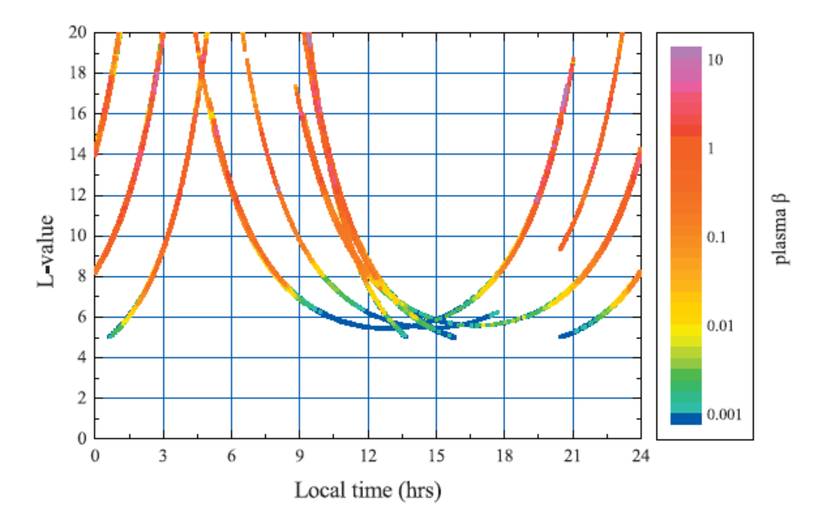

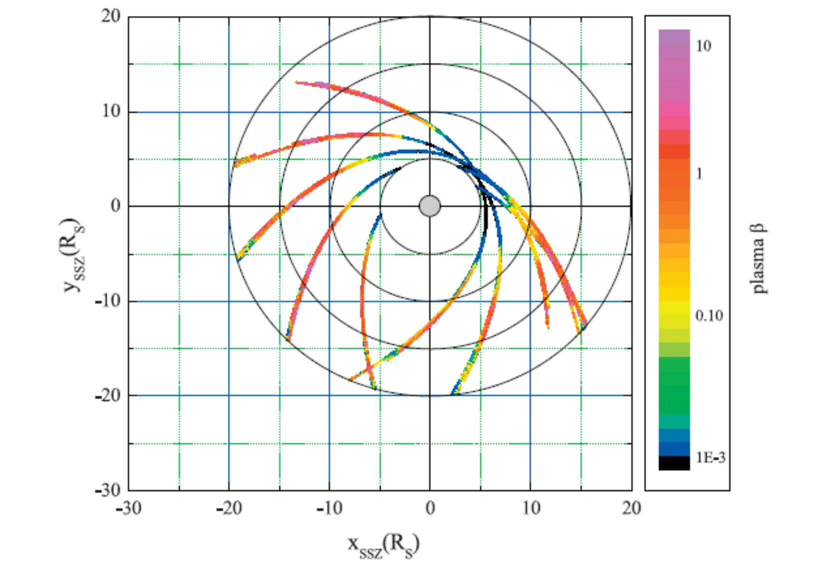

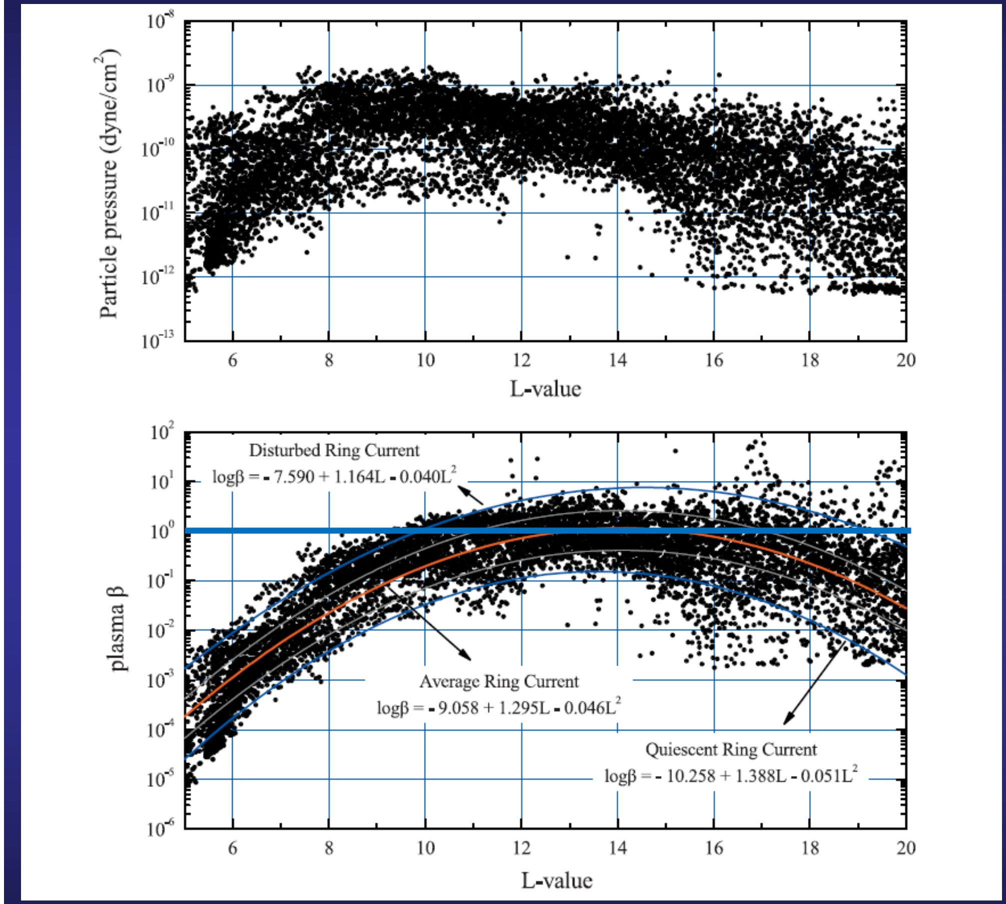

Summary

- will follow

Acknowledments

- Many thanks to:

M. Fränz, J. Woch, T. Wiegelmann, E. Marsch, R. Kallenbach, E. Roussos,

H. Koskinen

for providing material for those lecture.